

UCSF

UC San Francisco Electronic Theses and Dissertations

Title

Distinct roles of Bendless in regulating FSC niche competition and daughter cell differentiation

Permalink

<https://escholarship.org/uc/item/62v0s8n8>

Author

Tatapudy, Sumitra Devi

Publication Date

2021

Peer reviewed|Thesis/dissertation

Distinct roles of Bendless in regulating FSC niche competition and daughter cell differentiation

by
Sumitra Tatapudy

DISSERTATION
Submitted in partial satisfaction of the requirements for degree of
DOCTOR OF PHILOSOPHY

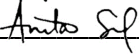
in

Genetics

in the

GRADUATE DIVISION
of the
UNIVERSITY OF CALIFORNIA, SAN FRANCISCO

Approved:

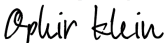
DocuSigned by:

58A91F5B7F204A2... Anita Sil
Chair

DocuSigned by:

452... Todd Nystul

DocuSigned by:

452... Jeremy Reiter

DocuSigned by:

4B3... F985C63D8CE3437... Ophir Klein

Committee Members

Dedication

I dedicate my dissertation work to my grandmother (*Ammamma*), Smt. Lalitha Gurunadham. Her penchant for learning and seeking knowledge has inspired me, and I know that she would have been proud of this achievement. I also dedicate this achievement to my parents, who did everything they possibly could to ensure that my educational aspirations were fulfilled and empowered me with the strength to overcome challenges. This one is for and because of you.

Acknowledgements

I would like to thank my parents, Padma and Sekhar Tatapudy, for giving me unconditional love, finding ways to support me throughout my education, teaching me to see opportunity instead of challenges, and for being the best sounding boards through my toughest periods in graduate school. I thank my sister, Sneha, for being a constant source of inspiration in how to overcome the toughest of challenges. Our laughs, experiences, songs together reminded me that I was a person outside of science – something that enabled me to enjoy the process! I am grateful for my husband, Sandheep, who has been the biggest source of strength through this journey. I cannot imagine these last couple of years of graduate school without your tremendous love and support. I am appreciative of UCSF since it helped me meet him!

Thank you to all my friends whose encouragement through all the different phases of my PhD has been so impactful. I would especially like to thank my friends, Navya, Rucha, Priam, and Satyaditya, since you have kept me afloat in so many ways through graduate school. Without your love, friendship, unwavering interest in understanding my science (despite not having a background in the subject), and commitment to creating moments of joy and ensuring that I was alright, I don't know how I could have achieved this. Without your friendship, Seema, the emotional ups and downs of graduate school would have been so much harder – I appreciate all our meals together, the trips you made to see me just to make sure all was well, and importantly, our conversations. Anuhya, you ensured I had fun, ate, slept and danced throughout the first couple of years of graduate school without getting consumed by the rigors of the program. I appreciate all of it.

I would like to thank my cohort-mates – I've learned so much for each one of you. Allison, Efren and Valentina, the group gatherings you hosted will forever be etched into my memory, since they really did bring all of us so much closer. Nneji, Karina and Efren, I think our first-year meetings cemented friendships that I was able to rely on through graduate school. Nick and Allison, our hangouts provided for such immense support throughout and great times while exploring restaurants in the Parnassus area! Our cohort is special, with every person having contributed to enriching this graduate school experience – thank you all for being you!

I would like to thank the Office of Career and Professional Development at UCSF, for providing me with tools and opportunities to explore my career interests, and identify science education as my future career path. Laurence Clement, you have been a fantastic role model, an inspiration, and a great mentor. I'm so glad we got the chance to work together, and I will always be grateful to you for the opportunities you created to allow for me to explore my interests in science education. It has been an honor and pleasure to learn from you. Rachel Care, thank you for being a fantastic supervisor through all my projects and before that, an inspiring graduate student leader! You along with Naledi, James and Karen have contributed so much to making it possible for me to work on science and career education related projects seamlessly while pursuing graduate school.

I would like to thank all members of the Nystul lab for being instrumental in my growth as a scientist, and honestly, as a person! I appreciate my advisor, Todd Nystul, for being a great role model in so many ways!! Thank you for your mentorship. Marimar, we started our journey in the Nystul lab around the same time, and you've been a sister to me through all the trials and tribulations during my early years of graduate school. Katja, you've been an inspiration to me, both scientifically and as a person. I've learned so, so much from you! Thank you for being a fantastic scientist, mentor and friend. Nate, Jobelle, Adriana and Ariane -- all your understanding, the laughs, dinners and coffee breaks contributed to so much contentment and happiness throughout graduate school – thank you! Every member in the Nystul lab, past and present, has taught me something significantly important. The Nystul lab community has been such caring and thoughtful space to work. Thank you to all past and present Nystulites who continue to make the space so collaborative, thoughtful and filled with “Aha!” moments.

A gratitude filled thank you to the broader UCSF community that is filled with so much collaborative spirit, care and commitment to be better. The influences of this intellectually stimulating community and an army of supportive people along the way have contributed immensely to my personal and scientific identity. Thank you all.

Distinct roles of Bendless in regulating FSC niche competition and daughter cell differentiation

Sumitra Tatapudy

Abstract

A major goal in the study of adult stem cells is to understand how cell fates are specified at the proper time and place to facilitate tissue homeostasis. Here, we found that an E2 ubiquitin ligase, Bendless (Ben), has multiple roles in the *Drosophila* ovarian epithelial follicle stem cell (FSC) lineage. First, Ben is part of the JNK signaling pathway, and we found that it, as well as other JNK pathway genes, are essential for differentiation of FSC daughter cells. Our data suggest that JNK signaling promotes differentiation by suppressing the activation of the EGFR effector, ERK. Also, we found that loss of ben, but not the JNK kinase hemipterous, resulted in an upregulation of hedgehog signaling, increased proliferation and increased niche competition. Lastly, we demonstrate that the hypercompetition phenotype caused by loss of ben is suppressed by decreasing the rate of proliferation or knockdown of the hedgehog pathway effector, Smoothened (Smo). Taken together, our findings reveal a new layer of regulation in which a single gene influences cell signaling at multiple stages of differentiation in the early FSC lineage.

Table of contents

Chapter 1:	1
1: Introduction and background.....	1
1.1 Stem cells.....	1
1.2 Epithelial stem cells and niches.....	2
1.3 Studying stem cells in vivo in <i>Drosophila</i>	2
1.4 The Follicle Stem cell (FSC) lineage.....	3
1.5 Signaling pathway activity in the <i>Drosophila</i> FSC lineage.....	4
1.6 Role of pHi in FSC differentiation.....	4
1.7 Studying hypercompetition in the FSC lineage.....	5
Chapter 2:.....	7
2: Intracellular pHi dynamics in the FSC lineage.....	7
Chapter 3:.....	11
3.1: E2 Ubiquitin ligase, bendless.....	11
3.2: Results.....	12
3.2.1 Bendless is required for follicle formation and stalk specification.....	12
3.2.2 JNK signaling is required for pFC differentiation.....	17
3.2.3 Loss of JNK signaling impairs the activation of Notch signaling pathway reporter.....	21
3.2.4 Impaired JNK signaling causes retention of phosphorylated ERK in pFCs, which blocks pFC differentiation	24
3.2.5 Ben functions in a JNK pathway independent manner to promote Hh signaling in FCs	30

3.2.6 Loss of Ben increases proliferation in pFCs.....	33
3.2.7 Loss of Ben causes hypercompetition in the FSC niche by regulating pFC proliferation and differentiation	37
3.3: Discussion	43
3.4: Future directions:.....	47
Chapter 4.....	48
4.1: Retinoblastoma factor, Rbf.....	48
4.1.1 Rbf is necessary for FSC differentiation	48
4.1.2 Loss of Rbf causes FSC hypercompetition.....	49
4.1.3 Loss of Rbf does not affect FC proliferation	50
4.2: Future directions:.....	51
Chapter 5.....	52
5: Materials and Methods	52
5.1 Fly husbandry and stocks	52
5.2 Immunostaining and imaging	52
5.3 EdU staining	53
5.4 EdU proliferative index analysis.....	54
5.5 Hybridization Chain Reaction	54
5.6 Clone induction.....	56
5.7 FSC competition assay	56
5.8 Statistics and graphs	56
6: References	57

List of figures

Figure 1.1: Schematic of germarium.....	3
Figure 2.1. Smoothened expression is not affected in FCs with increased pHi.....	9
Figure 2.2: Blocking an increase in pHi does not influence Hh pathway activity but Hh pathway activation causes an increase in pHi.....	10
Figure 3.1: <i>ben</i> and <i>hep</i> are broadly expressed in the germarium.....	13
Figure 3.2: <i>ben^A</i> clones exhibit a range of morphological phenotypes.....	14
Figure 3.3: Ben is required for stalk cell specification and follicle formation.....	15
Figure 3.4: JNK signaling is required for pFC differentiation and follicle formation.....	18
Figure 3.5: JNK signaling is required for follicle formation and stalk cell differentiation.....	19
Figure 3.6: Expression pattern of additional reporters for JNK signaling.....	20
Figure 3.7: JNK signaling does not affect the pattern of JAK-STAT signaling in the FSC lineage.....	21
Figure 3.8: JNK signaling is required for the normal expression of the Notch signaling reporter.....	23
Figure 3.9: JNK signaling is required to decrease pERK in pFCs.....	25
Figure 3.10: JNK signaling is required in pFCs to decrease pERK in pFCs.....	26
Figure 3.11: <i>ben^A</i> clones do not exhibit cell polarity defects.....	27
Figure 3.12: Constitutively active ERK in the FC lineage causes defects in stalk formation and differentiation.....	28
Figure 3.13: JNK pathway promotes FSC marker expression, Bin, in pFCs.....	29
Figure 3.14: Ben does not affect FSC marker, Wnt4, expression in FSCs.....	30
Figure 3.15: Ben is required for proper patterning of Hh signaling in the early FSC lineage.....	32
Figure 3.16: Loss of <i>ben</i> , but not <i>hep</i> causes increased proliferation in pFCs.....	35
Figure 3.17: Morphological phenotypes and proliferation of FCs in ovarioles with RNAi knockdown against E3 ligases and accessory proteins that interact with Bendless.....	37
Figure 3.18: Hypercompetition in <i>ben</i> mutant clones is suppressed by inhibition of proliferation or Hh signaling.....	40

Figure 3.19: Ovarioles with *ben^B* clones exhibit expanded pERK and tube-like phenotypes.....41

Figure 3.20: Proliferation and competition are not regulated by JNK component and E3 ubiquitin
ligase, Traf6, known to interact with Ben.....42

Figure 3.21: Increased proliferation can cause increased FSC competition in the niche.....42

Figure 3.22: Summary of the functions of Ben and JNK pathway genes in the FSC lineage.....46

Figure 4.1: Loss of Rbf results in differentiation defects.....49

Figure 4.2: *rbf^A* mutant FSCs are hypercompetitive and not overproliferative.....50

Chapter 1

Introduction and background

Stem cells

Multicellular organisms are composed of trillions of specialized cells with diverse functions. Stem cells are unspecialized cells, able to self-renew and differentiate into specialized cells in an organism. Given the multitude of functionalities for stem cells, research contributing to the characterization and implementation of stem cell therapies has been the focus of several investigations.

When a stem cell divides, it can self-renew or differentiate into more specialized cells. Depending on the potential for differentiation, stem cells are classified as being totipotent, pluripotent or multipotent. Totipotent stem cells are able to divide and differentiate into cells for the whole organism. A zygotic cell, which divides to produce all the different cell types in an organism, is an example of a totipotent stem cell. Pluripotent stem cells, like embryonic cells, have the potential to differentiate into the three germ layers -- ectoderm, mesoderm and endoderm -- but not extra embryonic tissue like the placenta. Therefore, they are able to differentiate into fewer cell types than totipotent cells. Multipotent cells, like adult stem cells, have a narrower differentiation spectrum than pluripotent stem cells and retain the ability to differentiate into discrete cells in specific cell lineages ([Zakrzewski et al. 2019](#)). In *Drosophila*, there is no pluripotent stem cell population. However, due to their genetic tractability and simple tissue architecture, *Drosophila* has been used as a model to study multipotent adult stem cells. Several well-characterized stem cell models in *Drosophila* include germline stem cells, intestinal stem cells, follicle stem cells (in females) and the somatic cyst stem cells (in males).

Epithelial stem cell niches

Adult stem cells play a critical role in maintaining tissue homeostasis in response to environmental insults and injury often leading to cell damage and death. Many epithelial tissues of the human body are maintained by adult epithelial stem cells including the intestine, breast, brain, lung, hair, and others (Blanpain et al., 2007; Gonzalez-Perez, 2012; Donne et al., 2015). Stem cells divisions can result in the production of stem cells or daughter cells that differentiate into more specialized cell types. A healthy population of stem cells maintains a homeostatic balance between self-renewal and differentiation; however, when stem cells are dysregulated it can disrupt this homeostatic balance leading to the overproduction of stem cells or differentiating cells. Previous studies have proposed that stem cell mutagenesis, abnormal proliferation or differentiation can determine organ cancer risk (La Marka et al., 2020, Doupe, D.P., et al. 2012). Therefore, since the dysregulation of stem cells has been proposed as being causative in the formation of cancer, understanding the regulation underlying stem cell functionality and dynamics is necessary.

Studying stem cells in vivo in *Drosophila*

Adult stem cells reside in the niche, specialized microenvironments that are responsible for maintaining stem-like potential and activity. In the *Drosophila* model system, the most well-characterized adult epithelial stem cell lineages include the follicle stem cell lineage and the intestinal stem cell lineage. In these models, epithelial stem cells exit the niche and further differentiate into more specialized cell types. The benchmark for identifying stem cells is using lineage analysis, in which stem cells are labeled with a genetically heritable marker and patterns of marker inheritance by cells are observed over time. Other than this functional assay, one of the challenges with studying these epithelial stem cell lineages has been the lack of markers that accurately identify stem cells and transit amplifying cells. Further, this presents a need to understand the regulation underlying transitions from stem cell like fate to transit amplifying cells.

The Follicle Stem Cell (FSC) lineage

The follicle epithelium of the *Drosophila* ovary is a tractable model for studying the mechanisms that govern cell fate transitions in an epithelial stem cell lineage (Rust and Nystul, 2020). The *Drosophila* ovary is made up of approximately 16 strands of developing follicles called ovarioles (Miller, 1950). Follicle production begins at the anterior tip of the ovariole in a structure called the germarium, which is divided into four regions based on the stages of germ cell development. New germ cells are produced by germline stem cells in Region 1 and undergo four rounds of synchronous division to become a 16-cell cyst of interconnected cells as they move into Region 2a (Carpenter, 1975; Koch and King, 1966). Germ cells then encounter the follicle epithelium at the border between Regions 2a and 2b where the FSCs reside. FSCs produce a transit amplifying population of cells called pre-follicle cells (pFCs), which associate with germ cells as they enter Region 2b and begin to differentiate into one of three main cell types: polar cells, stalk cells, or main body follicle cells (Fig. 1.1).

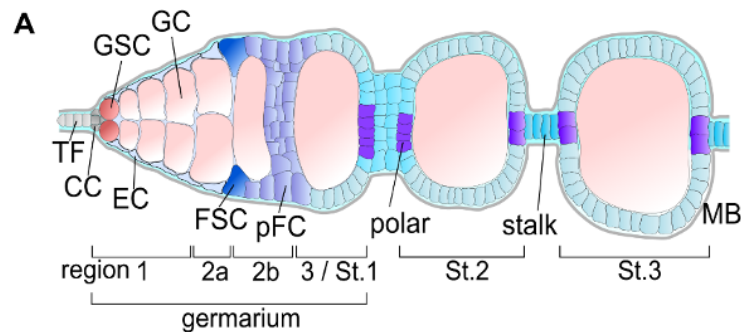


Figure 1.1. Schematic of the germarium. (A) Schematic of the germarium depicting terminal filament cells (TF), cap cells (CC), germline stem cells (GSC), germ cells (GC), in region follicle stem cells (FSC), pre-follicle cells (pFC), polar, stalk and main body follicle cells (MB). The germarium is divided into Region 1, Region 2a (2a), Region 2b (2b) and Region 3 (3), which is also called Stage 1 (St. 1). The first and second fully budded follicles are referred to as Stage 2 (St. 2) and Stage 3 (St. 3) respectively.

Signaling pathway activity in the *Drosophila* FSC lineage

A defining feature of adult stem cells is the ability to self-renew while producing daughters that differentiate into functional cell types in the tissue. This segregation of stem cell and daughter cell fates

requires the coordinated action of multiple self-renewal and differentiation signals to ensure that each cell acquires the proper fate. It is likely that newly produced daughter cells need to both reduce response to niche signals and upregulate differentiation cues to differentiate properly, but how the transition from a stem cell identity to a differentiating daughter cell identity is regulated is not well-understood.

FSC self-renewal is controlled by several signaling pathways, including EGFR, Wnt and Hedgehog (Hh), which are active in the FSCs and must be downregulated in newly-produced pFCs for differentiation to occur (Castanieto et al., 2014; Hartman et al., 2013; Huang and Kalderon, 2014; Johnston et al., 2016; Kim-Yip and Nystul, 2018; Melamed and Kalderon, 2020; Sahai-Hernandez and Nystul, 2013; Singh et al., 2018; Song and Xie, 2003; Zhang and Kalderon, 2000; Zhang and Kalderon, 2001). In pFCs, activation of Notch signaling in response to a Delta signal from germ cells initiates differentiation toward the polar cell fate (Dai et al., 2017; Lopez-Schier and St Johnston, 2001; Nystul and Spradling, 2010). Polar cells activate JAK/STAT signaling in neighboring cells, inducing a stalk cell fate, and the pFCs that do not become polar or stalk cells differentiate into main body follicle cells (Assa-Kunik et al., 2007; Dai et al., 2017).

Role of pHi in FSC differentiation

Mounting evidence demonstrates that transient changes in pHi dynamics can act as cytosolic signals that contribute to the regulation of cell cycle progression (Putney and Barber, 2003; Schreiber, 2005), membrane trafficking (Mukherjee et al., 2006; Brown et al., 2009; Kojima et al., 2012), and cell-substrate adhesion (Srivastava et al., 2008; Choi et al., 2013). pHi has also been found to be dysregulated in some diseases, such as cancer (Webb et al., 2011; Parks et al., 2013) and neurodegenerative disorders (Harguindey et al., 2007; Wolfe et al., 2013). A previous study from the Nystul lab demonstrated that pHi increases as FSCs differentiate into during the differentiation of FSCs and mouse ESCs and is necessary differentiation into specialized cell types in both these lineages. Additionally, the study identified a specific role for pHi dynamics in the regulation of Hedgehog (Hh) signaling in the FSC lineage, however the precise mechanism by which pHi dynamics were regulated in the FSC lineage remained less understood. This

discovery laid the foundation for understanding the mechanism by which cytosolic cues instruct cell fate decisions. Specifically, these findings piqued my interest in deciphering the role that pHi plays in instructing cell fate decisions as FSCs transition into pFCs, a previously less characterized transition state.

Studying hypercompetition in the FSC lineage

FSCs commonly divide with asymmetric outcomes to self-renew and produce a pFC, but can also divide symmetrically, for example, during FSC loss and replacement events (Kronen et al., 2014; Margolis and Spradling, 1995; Wang et al., 2012). This suggests that the fate of the FSC daughter cells is not specified at the time of division, but the regulation of these decisions is not fully understood. In a WT tissue, since both stem cells are equally fit, there is no bias favoring the replacement of one stem cell over another. However, a previous study for the Nystul lab established a genetic basis for the regulation of FSC replacement in the niche. In this study, certain mutations in FSCs led to FSCs gaining a competitive advantage or disadvantage causing mutant FSCs to be more likely to outcompete WT cells or get replaced by WT cells respectively. These mutant phenotypes are referred to as hypercompetition and hypocompetition, respectively. This study included the results from a screen through 126 recessive lethal mutations from a collection of alleles on the X-chromosome. All alleles contained mutations that were not cell lethal, but organismal lethal, produced a scorable phenotype in adult tissue and contained a mutation in a single gene that could be rescued by genomic duplication.

One strategy to understand the regulation of FSC to differentiated cell state transitions has been to identifying mutations that skew the balance between self-renewal and differentiation by conferring a competitive advantage or disadvantage for niche occupancy and thereby affecting the rate of FSC loss and replacement (Cook et al., 2017; Kronen et al., 2014; Wang et al., 2012). Consistent with this, a previous study found that *lgl* and *dlg* mutant FSCs were hypercompetitive and the mutant tissue displayed differentiation defects. While associations between differentiation defects and competition phenotypes have been noted for several other hyper- and hypo- competition candidates, a systematic investigation into the

regulatory mechanism for FSC competition had not been done. Given my interest in identifying processes that enhance differences between self-renewing and differentiating daughter cells, through my thesis research, I took on the opportunity to study stem cell fitness as a means to identify mechanisms that might contribute to establishing asymmetry between FSCs and pFCs. From a therapeutic standpoint, previous studies suggest that mutations that increase stem cell competition, or hypercompetitive alleles, cause the clonal expansion of a mutant stem-like lineage to form fields that are pre-disposed to tumor development called pre-malignant fields (Slaughter, D. P., et al., 1953, Buczacki, S. J. A., et al., 2013, Braakhuis, B. J. M., et al., 2003). Therefore, understanding the rules that govern stem cell competition will be important for the development of new diagnostics and therapeutics for cancer and stem-cell based diseases.

My doctoral work was motivated by the following questions:

1. How do changes in pHi instruct the transition from FSC to pFC state?
2. What are the mechanisms that cause mutant FSCs to remain in the niche and outcompete WT FSCs?

Chapter 2:

Intracellular pHi dynamics in the FSC lineage

When an adult stem cell divides, one daughter retains its stem cell identity and the other daughter loses its self-renewal capacity and differentiates. The precise mechanisms that govern these asymmetric cell fate decisions are poorly understood. Adult stem cells reside in a specialized microenvironment: the stem cell niche. Niche signals are thought to play a role in stem cell fate specification and maintenance during development. The epithelial follicle stem cell lineage of the *Drosophila* ovary has proven to be an excellent model system to understand the complex interplay between in vivo niche signals and their impact on cell fate decisions.

Until recently, the role of intracellular pH (pHi) in regulating cell fate differentiation decisions, was largely unexplored. pHi homeostasis is tightly regulated in most tissues to remain within the range of 7.2 to 7.4 (Webb, B.A., et al., 2011). The major buffering system in cells is the CO₂-Bicarbonate buffering system (Casey, J.R. et al., 2009). Since many pHi fluctuations occur in response to intracellular processes, pHi homeostasis is maintained by the activity of proton transporters from the Solute Carrier (SLC) family of genes. Proton transporters can be divided into two main classes - acid extruders, which export H⁺ or import HCO₃⁻, and acid loaders which import H⁺ or export HCO₃⁻. Acid extruders commonly include Na⁺/H⁺ exchangers (NHE) whereas acid loaders commonly include Cl⁻/HCO₃⁻ transporters (Casey, J.R. et al., 2009). Maintaining pHi homeostasis requires intracellular pH sensors. Many pH-sensitive molecules participate in a variety of cellular processes that include metabolism, vesicle trafficking⁴, cell communication⁶⁻⁸, ion homeostasis⁹, and cell motility¹⁰⁻¹² (Erecińska, M. et al., 1995, Casey, J.R. et al., 2009, Ek-Vitorín, J. F., 1996, González-Nieto, D., 2008, Chen, Y., 2000, Waldmann, R., 1999, Denker, S. P. et al., 2002, Frantz, C., 2008, Denker, S. P., 2000). A few examples of pH sensors include phosphofruktokinase, a key glycolytic enzyme that serves as a checkpoint for glycolysis, adenylate cyclase, and cofilin, involved in actin remodeling (Erecińska, M. et al., 1995, Chen, Y, 2000, Frantz, C.,

2008). When pHi homeostasis is disrupted, proton transporters are differentially regulated to achieve homeostasis.

Recent findings from our lab indicate that pHi increases as follicle stem cells differentiate into pre-follicle cells preFCs and further into FCs, thereby establishing a pHi gradient as differentiation proceeds (Ulmschneider et al., 2016). Additionally, maintaining a specific pHi is necessary during differentiation since genetically altering pHi results in differentiation defects (Ulmschneider et al., 2016). Additionally, preliminary data suggests that an increase in pHi causes a decrease in Hedgehog (Hh) signaling (Ulmschneider et al., 2016). However, the mechanism by which pHi attenuates Hh signaling is less understood. **Therefore, I began to investigate the mechanism by which pHi regulates FSC differentiation.**

In canonical Hh signaling, the Hh ligand activates its receptor, Patched (ptc). This causes ptc to relieve its inhibitory effect on Smoothed (Smo), a G-protein-coupled receptor, causing smo activation and the subsequent activation of Ci, a transcription factor of Hh target genes like ptc, dpp, engrailed (en). Preliminary data in the lab has suggested that overexpression of DNhe2 caused lower smo-GFP expression throughout the FSC lineage. However, I was not able to confirm these results based on the image analysis and quantifications performed on germaria expressing smoGFP and 109-30>UAS-smoGFP in control and in germaria overexpressing DNhe2 under the control of FC driver 109-30 (Fig. 2.1).

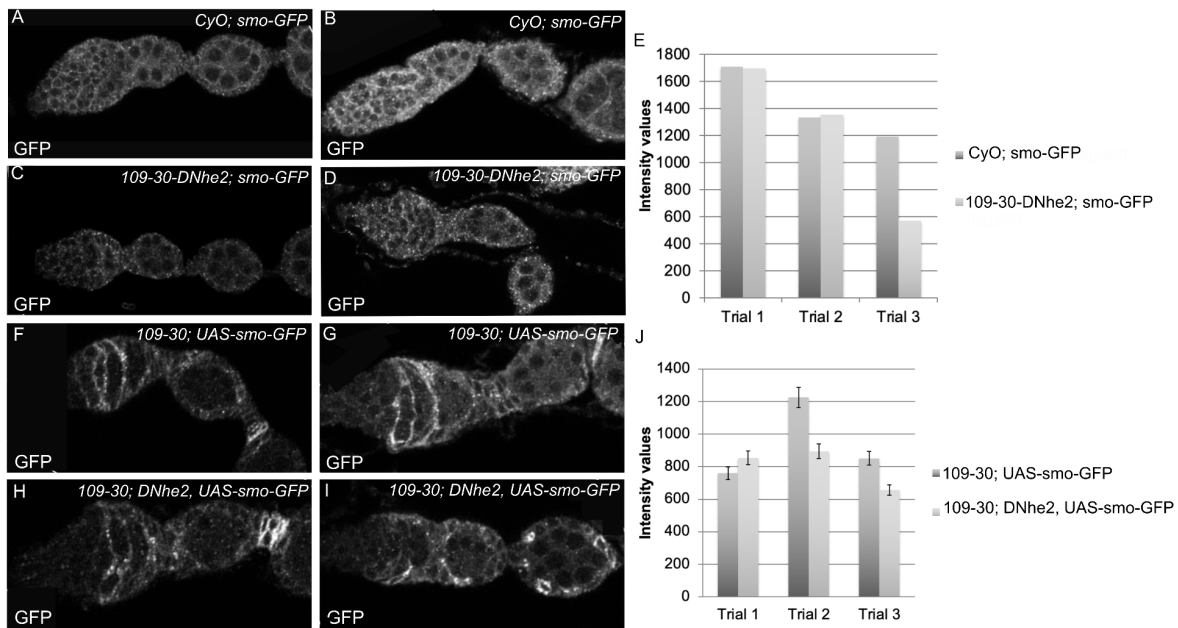


Figure 2.1. Smoothened expression is not affected in FCs with increased pHi

(A-D) Images depicting smo-GFP expression in Control (CyO; smo-GFP) and ovarioles overexpressing DNhe2 under the control of 109-30^{ts}. (E) Quantification of smo-GFP intensity in control and ovarioles overexpressing DNhe2 under the control of 109-30^{ts}. (F-I) Images depicting 109-30^{ts} driving UAS-smo-GFP expression in Control (CyO; 109-30^{ts}>UAS-smo-GFP) and ovarioles overexpressing DNhe2. (J) Quantification of UAS-smo-GFP intensity in control and ovarioles overexpressing DNhe2 under the control of 109-30^{ts}.

After this, I shifted my focus towards identifying other pHi sensitive proteins that might act as sensors in the Hh signaling pathway. We found an inverse correlation between pHi and Hh pathway activity in the FSC lineage. (As pHi increased, Hh pathway activity decreased measured by ptc-GFP. An increase in pHi also partially rescued ptc-RNAi morphological and differentiation defects). Motivated by these results, we asked whether the effect of pHi on Hh pathway activity is generalizable to other model systems. In order to study the mechanism by which pHi affects Hh signaling, we intended to identify a cell-based model system, that was straightforward to use for biochemical and immunofluorescence experiments. To answer this question, we asked whether pHi effects Hh pathway activity in *NIH-3T3* cells, a mammalian cell line commonly used to study Hh signaling.

We aimed to increase pHi in *NIH-3T3* cells and measure the effect on targets of Hh signaling, Gli and Patched using qRT-PCR (Fig. 2.2). We first measured pHi and gli, ptc transcript levels in 3T3 cells

with and without Hh pathway agonist, SAG. While we did not expect a change in pHi between these conditions, we found that activating the pathway increases pHi. So, this presented a natural scenario to test the effect of pHi on Hh activity. We planned to inhibit the increase in pHi using EIPA, a chemical that blocks proton exchanger NHE-1, in both Hh activated and inactivated conditions and measure gli, ptc transcript levels. We hypothesized that inhibiting the pHi increase in a Hh activated condition would be correlated with reduced levels of Gli and Ptc mRNA levels, detected by qRT-PCR. However, we found no significant change in gli, ptc transcription when pHi increase was inhibited with EIPA, indicating that pHi does not regulate Hh signaling in *NIH-3T3* cells.

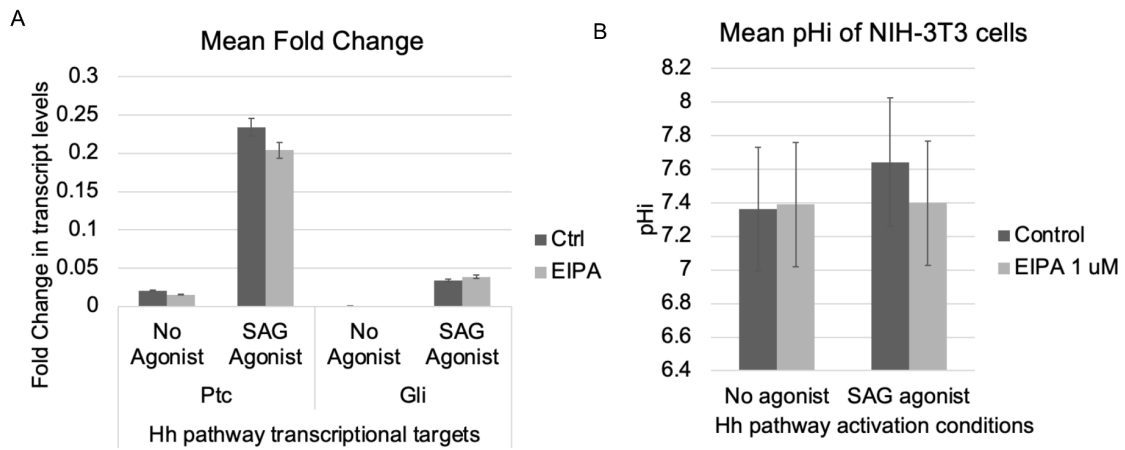


Figure 2.2: Blocking an increase in pHi does not influence Hh pathway activity but Hh pathway activation causes an increase in pHi.

(A) qRT-PCR mean fold change in Hh pathway targets, ptc and gli. (B) pHi measurements upon Hh pathway activation and inactivation. In addition, pHi measurements when EIPA, a chemical that inhibits NHE-1 activity, is used to block increase in pHi.

Future directions:

An interesting finding that emerged through these efforts was that pHi naturally increased when the SAG agonist was added to activate the Hh signaling pathway. This was an intriguing finding; while suppressing the increase in pHi did not affect the Hh pathway itself, it would be interesting to determine the functional relevance of increased pHi due to Hh pathway activation in *NIH-3T3* cells (Fig. 2).

Chapter 3:

E2 Ubiquitin ligase, *bendless*

Recently, we reported the results of a forward genetic screen for FSC niche mutants (Cook et al., 2017). Among the strongest hits from the screen was an allele of *bendless* (*ben*), which is an E2 ubiquitin ligase that is a core component of the JNK pathway (Ma et al., 2014). The allele, *ben^A*, contains a single nonsense mutation in the C-terminal domain of the protein and is homozygous lethal. We reported that FSC clones that are homozygous for *ben^A* were more abundant than controls, suggesting that it causes FSC niche hypercompetition (Cook et al., 2017). However, this was not confirmed and the cause of this phenotype and the specific roles of *ben* in the early FSC lineage were not investigated.

First characterized in its role in facilitating normal synaptic connections in the *Drosophila* brain, Ben has been known to interact with multiple E3 ligases to facilitate K63 linked polyubiquitination which usually results in activation of signaling pathways. Bendless interacts with E3 Ubiquitin ligase Traf2/6 to positively regulate JNK signaling and Imd signaling, E3 Ubiquitin ligase Nopo to preserve genomic integrity during early *Drosophila* embryogenesis, E3 Ubiquitin ligase accessory factor *DREDD* to regulate IMD signaling, E3 Ubiquitin ligase CG14435 (although the downstream function of this interaction is unknown).

In this study, we identify multiple, genetically distinct roles for *ben* in the early FSC lineage. First, we demonstrate that *ben* and other core components of the JNK pathway are required for specification of the stalk cell fate. Second, we show that *ben* regulates the level of Hh signaling and the rate of proliferation in pFCs, whereas the downstream JNK pathway component, *hemipterous* (*hep*) does not. We also provide evidence that *ben*, but not JNK signaling, may contribute to the specification of the main body cell fate at this stage. In addition, we test the association between hypercompetition, increased proliferation, and Hh signaling in *ben^A* mutants, and find that overexpression of the cell cycle inhibitor, *dacapo* (*dap*) or reduction of the Hh pathway effector, *smoothened* (*smo*) is sufficient to suppress the hypercompetition phenotype.

However, we show that *hep* mutant clones are not hypercompetitive, indicating that hypercompetition of *ben^A* mutant clones is a JNK-independent effect. Taken together, these findings demonstrate that *ben* has distinct roles in the regulation of proliferation and differentiation in the FSC lineage and that a layer of regulation exists that acts to both downregulate niche signals in newly-produced pFCs and promote the activation of differentiation cues.

Results

***Bendless* is required for follicle formation and stalk cell specification**

To investigate the function of *ben* in the early FSC lineage, we first determined the expression pattern of *ben* in the ovary. We found that *ben* RNA is detectable in all cell types that were profiled in our recent ovarian cell atlas (Fig. 3.1A) (Rust et al., 2020). To confirm this *in vivo*, we assayed for *ben* transcripts in the germarium using fluorescence in situ hybridization chain reaction (HCR) (Choi et al., 2018) and, indeed, we observed that *ben* is broadly expressed, including in FSCs and pFCs. This signal was substantially reduced in follicle cells with the expression of *ben[RNAi]* using the early follicle cell Gal4 driver, *109-30-Gal4* (Hartman et al., 2010), which indicates that the signal is specific for *ben* transcripts and confirms that the RNAi line is effective (Fig. 3.1B-C).

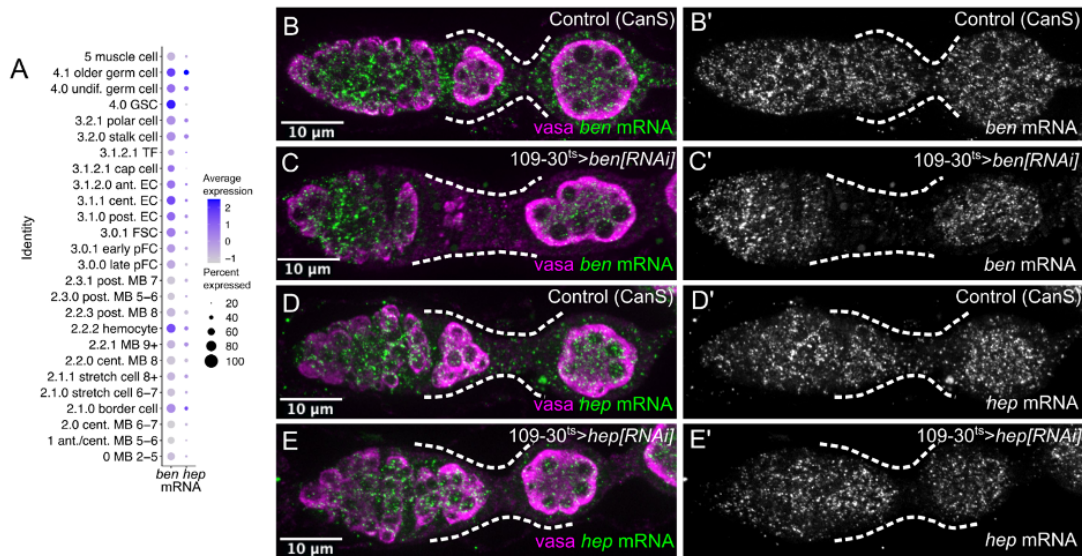


Figure 3.1. *ben* and *hep* are broadly expressed in the germarium.

(A) Dotplot showing the expression of *ben* and *hep* mRNA detected in each cell type by single cell RNA sequencing of the ovary (Rust, et al., 2020). (B-E) Ovarioles from Canton-S (CanS) flies (B and D) or with $109-30^{ts}$ driving *ben[RNAi]* or *hep[RNAi]* stained for *ben* or *hep* transcripts using HCR (green) and Vasa (magenta). The HCR channel is shown separately in B'-E'. $109-30-Gal4$ is expressed in follicle cells within the germarium (white dashed lines) (Hartman et al., 2010; Sahai-Hernandez and Nystul, 2013) absence of signal in these cells in C and E confirms that the HCR probes are specific for their target transcripts and that the RNAi lines are effective in knocking down mRNA expression.

Next, we stained ovarioles with wild-type or *ben^A* clones that are marked by the lack of GFP (GFP⁻) for Fas3, which marks membranes of early follicle cells, and examined the tissue morphology. We found that ovarioles in which the follicle cell population in the germarium was mosaic (partially marked) or only consisted of *ben^A* mutant cells (fully marked) had a range of follicle formation defects, including gaps in the follicle epithelium, “tube-like” phenotypes characterized by defective or absent stalks between the germarium and the downstream follicles, and “expanded stalk” phenotypes characterized by the presence of extra cells in the stalk region that form multiple rows (Fig. 3.3B-D, K and Fig. 3.2A-D) (Berns et al., 2014). We also noticed a small but significant increase in the frequency of ovarioles with follicle formation defects in *ben^A/+* heterozygous flies compared to wild-type controls (Fig. 3.2E), but the frequencies of follicle formation phenotypes were not significantly different between *ben^A/+* ovarioles with or without

ben^A homozygous germ cell clones (Fig. 3.2E). This suggests that *ben* is not required in germ cells for follicle formation. We observed similar phenotypes in ovarioles with *ben[RNAi]* driven in early follicle cells specifically during adulthood using *109-30-Gal4* and *tub-Gal80^{ts}* (McGuire et al., 2003) (referred to hereafter as *109-30^{ts}*), though the expanded stalk phenotype was more common in this context (Fig. 3.3E-G and Fig. 3.3L). This confirms that reduction of *ben* expression in the early FSC lineage causes follicle formation defects.

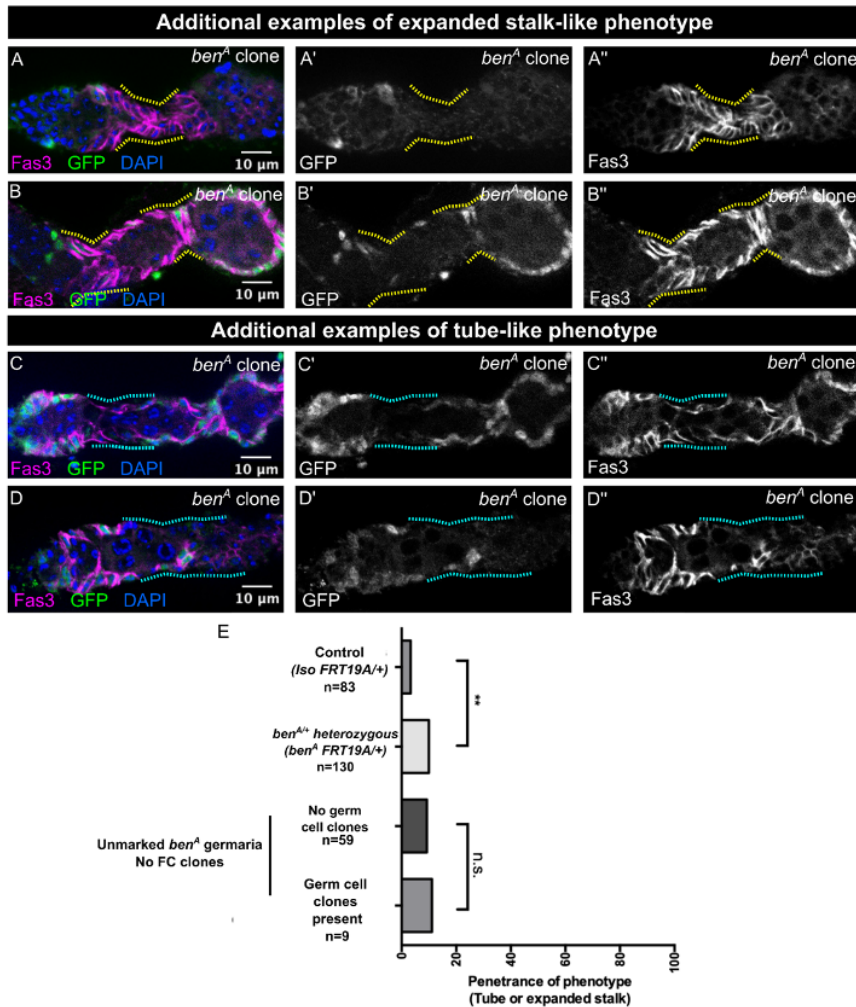


Figure 3.2: *ben^A* clones exhibit a range of morphological phenotypes.

(A-D) Ovarioles with GFP- *ben^A* clones stained for Fas3 (magenta), GFP (green), and DAPI (blue). Expanded stalk (yellow dotted lines) and tube-like phenotypes (cyan dotted lines) are indicated. (E) Quantification of the frequency of ovarioles with either and expanded stalk or tube-like phenotype in wildtype control (*IsoFRT19A/+*), *ben^{A/+}* heterozygous (*ben^A, FRT19A/+*), and “unmarked” *ben^A* germaria

(*ben^A, FRT19A/hsFlp, Ubi-GFP, FRT19A*) that do not have any follicle cell (FC) clones but either do or do not germ cell clones. Chi-squared test, ** = $p < 0.01$, n.s. = not significant, n (number of ovarioles examined) are indicated in (E).

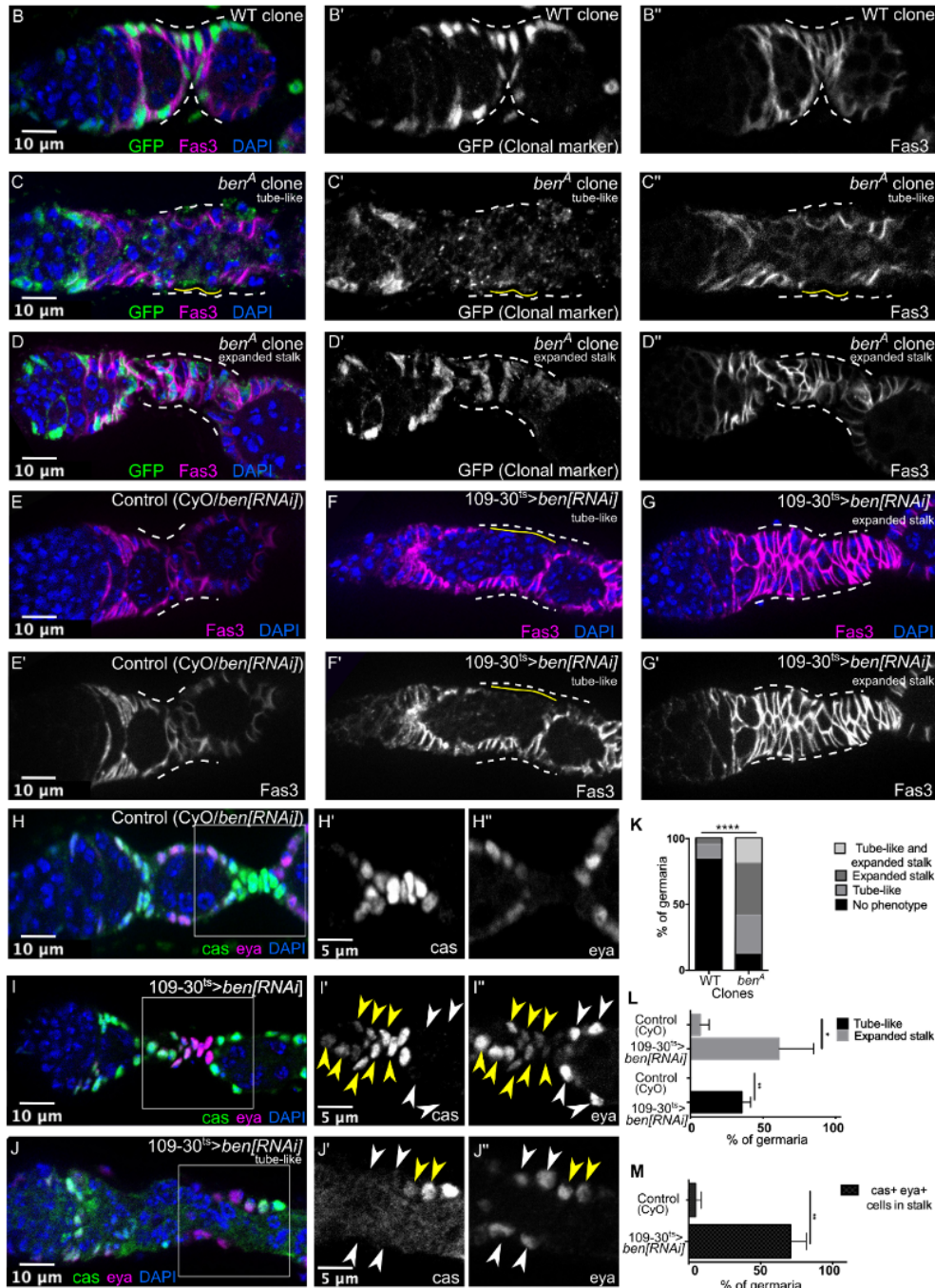


Figure 3.3. Ben is required for stalk cell specification and follicle formation.

(B-D) Ovarioles with wild-type (WT) or *ben^A* GFP⁻ clones stained for Fas3 (magenta), GFP (green), and DAPI (blue). In wild-type ovarioles, stalk cells form into a single row of cells between adjacent follicles. In ovarioles with *ben^A* clones we observed gaps in the follicle epithelium (yellow lines), and the stalk regions can be absent, causing adjacent follicles to merge together (“tube-like phenotype”, C) or cells can accumulate in this region and fail to intercalate into a single row (“expanded stalk phenotype”, D). In all cases, the clones extend well beyond the germarium, and the ovarioles are mosaic or fully marked by the lack of GFP. (E-G) Ovarioles with *ben[RNAi]* over a CyO balancer (Control) (E) or with *109-30^{ts}* driving expression of *ben[RNAi]* (F-G) stained with Fas3 (magenta) and DAPI (blue). The stalk regions in panels B-G are indicated with white dashed lines. (H-J) Ovarioles with *ben[RNAi]* alone (H) or with *109-30^{ts}* driving expression of *ben[RNAi]* (I-J) stained for Eya (magenta), Cas (green) and DAPI (blue). In control germaria, stalk cells are Cas⁺ Eya⁻ and main body cells are Cas⁻, Eya⁺ (H). With knockdown of *ben*, the main body cells are still Cas⁻, Eya⁺ (white arrowheads), but there are Cas⁺, Eya⁺ cells in the stalk region (yellow arrowheads) (I, J). (K) Quantification of the frequency of germaria with tube-like and expanded stalk phenotype in ovarioles with mosaic or fully marked WT and *ben^A* mutant clones. Chi-squared test: **** = p<0.0001, n.s = not significant, n≥68 ovarioles. (L) Quantification of the frequency of germaria with tube-like and expanded stalk phenotype in germaria with *ben[RNAi]* alone or *109-30^{ts}* driving expression of *ben[RNAi]*. Student’s t-test: ** = p<0.01, * = p<0.05, n.s. = not significant, N=3 flies, n≥84 ovarioles. (M) Quantification of the frequency of germaria with Cas⁺, Eya⁺ in the stalk region in germaria with *ben[RNAi]* alone or *109-30^{ts}* driving expression of *ben[RNAi]*. Student’s t-test: ** = p<0.01, n.s. = not significant, N=3 flies, n≥79 ovarioles.

Since stalk cell specification is initiated in a subset of pFCs in the early FSC lineage, tube-like and expanded stalk phenotypes suggest a defect in pFC differentiation (Berns et al., 2014). To further assay for follicle cell differentiation defects upon knockdown of *ben*, we stained ovarioles with *ben[RNAi]* driven by *109-30^{ts}* for Castor (Cas) and Eyes absent (Eya). In control ovarioles, early pFCs express high levels of both Cas and Eya and then become either Cas⁺, Eya⁻ as they differentiate into stalk or polar cells, or Cas⁻, Eya⁺ as they differentiate into main body follicle cells (Fig. 3.3H) (Bai and Montell, 2002; Chang et al., 2013). We found that a majority (70.9% ± 10.9%, N=30) of ovarioles with *ben[RNAi]* driven by *109-30^{ts}* contained Cas⁺, Eya⁺ cells in the regions between follicles, where stalk cells typically reside (Fig. 3.3I-J, M). However, the main body follicle cells surrounding recently budded follicles in these mutant ovarioles were Cas⁻, Eya⁺ (Fig. 3.3I-J), indicating that, unlike the cells in the stalk region, they were able to exit the Cas⁺, Eya⁺ state associated with pFC identity. Taken together, these results suggest that the follicle formation defects caused by knockdown of *ben* are due, at least in part, to a failure of mutant pFCs to differentiate into stalk cells.

JNK signaling is required for pFC differentiation

Ben is a positive regulator of JNK signaling in the *Drosophila* eye and wing discs (Herrera and Bach, 2021; Ma et al., 2014), so we hypothesized that the follicle formation defects in *ben* mutants are due to impaired JNK signaling. JNK signaling is activated when a secreted ligand, Eiger (Egr), binds to a cell surface receptor, Grindelwald (Grnd) or Wengen (Wgn) to initiate a cascade of intracellular events (Fig. 3.5A). First, Ben and the E3 Ubiquitin ligase, TNF-receptor-associated factor 6 (Traf6), ubiquitinate the upstream kinase, TGF- β activated kinase 1 (dTAK1), which then phosphorylates and activates downstream kinases, Basket (Bsk) and Hep, ultimately leading to the activation of the transcription factor complex, AP-1 (Tafesh-Edwards and Eleftherianos, 2020). We found that *hep* RNA is expressed broadly throughout the germarium and early follicles (Fig. 3.1A, D-E) and that the synthetic JNK signaling reporter, AP-1-GFP (Chatterjee and Bohmann 2012; Harris et al. 2016), is detectable in escort cells and stalk cells (Fig. 3.4A). In ovarioles with *ben^A* follicle cell clones, AP-1-GFP expression was absent in stalk cells, indicating that Ben positively regulates JNK signaling in the FSC lineage (Fig. 3.4B).

To determine whether other components of the JNK pathway are required for follicle formation and early pFC differentiation, we depleted expression of Hep, Egr, Grnd or Bsk using RNAi in early follicle cells during adulthood and stained for Fas3. Indeed, knockdown of any of these genes caused both tube-like and expanded stalk phenotypes (Fig. 3.4C-F, 3.5B-G). To further confirm the requirement of Hep for stalk differentiation, we generated follicle cell clones that are homozygous for *hep^{G0107}*, which is a recessive lethal mutation (Baril et al., 2009; Guichard et al., 2006). Again, we observed ovarioles with tube-like and expanded stalk phenotypes (50.9%, Fig. 3.4G-H, 3.4K). Moreover, as with knockdown of *ben*, we observed cells within the expanded stalks of *hep[RNAi]* mutants that were still Cas⁺, Eya⁺, whereas the cells in the main body cell region had matured into the Cas⁻, Eya⁺ state (Fig. 3.4I-J, L). This suggests that RNAi knockdown of Hep impairs differentiation of pFCs into stalk cells. Collectively, these experiments confirm that Ben positively regulates JNK signaling in follicle cells, and that JNK signaling is necessary for pFC differentiation into stalk cells.

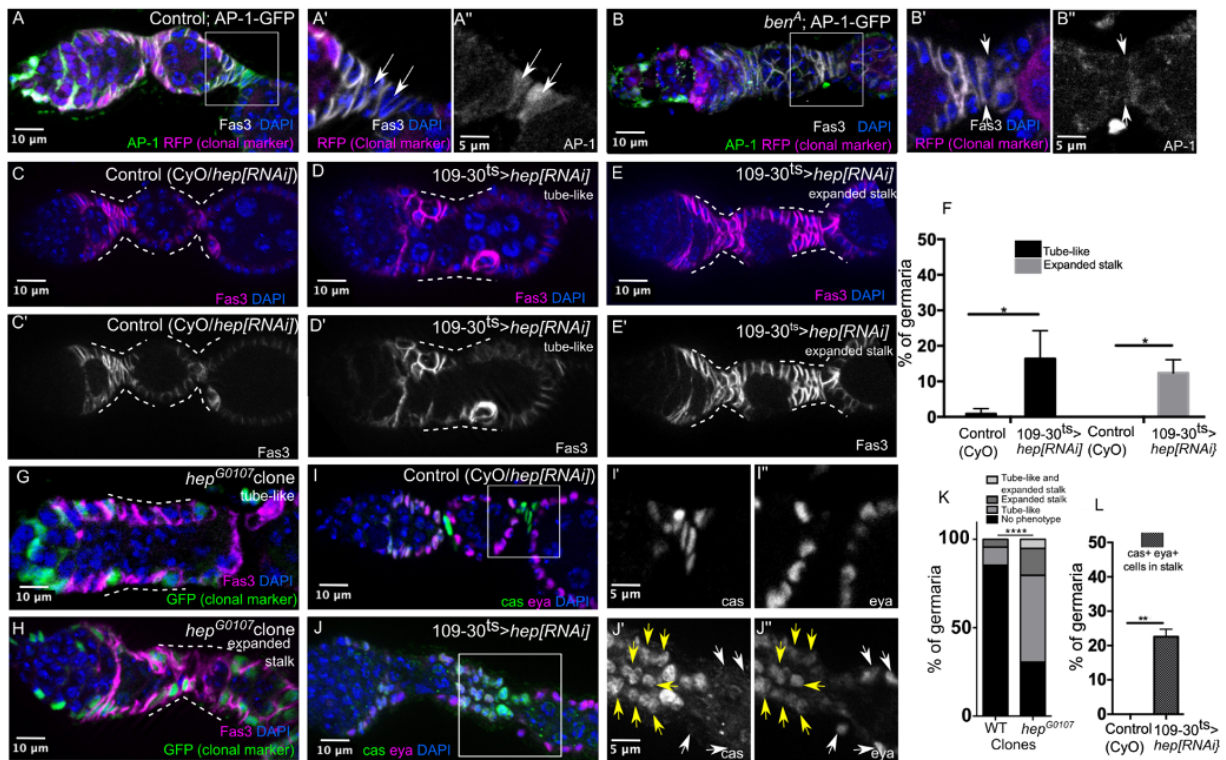


Figure 3.4. JNK signaling is required for pFC differentiation and follicle formation.

(A-B) Ovarioles with the *AP-1-GFP* reporter and wild-type control (A) or *ben^A* RFP⁻ clones (B) stained for Fas3 (white), RFP (magenta), GFP (green), and DAPI (blue). *AP-1-GFP* reporter activity is present in wild-type stalk cells but absent in *ben^A* stalk cells (white arrows). (C-E) Ovarioles with *hep[RNAi]* alone (C) or *109-30^{ts}* driving expression of *hep[RNAi]* (D-E) stained with Fas3 (magenta) and DAPI (blue). Wild-type stalk morphology is present in control ovarioles (white dashed line, C); tube-like stalk phenotype (white dashed line, D) and expanded stalk phenotype (white dashed line, E) are present in ovarioles with *109-30^{ts}* driving expression of *hep[RNAi]*. (F) Quantification of the frequency of germaria with tube-like and expanded stalk phenotype in germaria with *hep[RNAi]* alone or *109-30^{ts}* driving expression of *hep[RNAi]*. Student's t-test: * = $p < 0.05$, n.s. = not significant, $N = 3$ flies, $n \geq 84$ ovarioles. (G-H) Ovarioles with *hep^{G0107}* mutant clones stained for Fas3 (magenta), GFP (green), and DAPI (blue). Clones are marked by the lack of GFP. Tube-like phenotype (G) or expanded stalk phenotype (H) present in ovarioles with *hep^{G0107}* mutant clones. (I-J) Ovarioles with *hep[RNAi]* alone (I) or *109-30^{ts}* driving expression of *hep[RNAi]* (J) stained with Eya (magenta), Cas (green) and DAPI (blue). Control germaria contain *Cas⁺* *Eya⁻* cells in stalk region and *Cas⁻*, *Eya⁺* cells in main body cell region (I), whereas *Cas⁺*, *Eya⁺* cells in the stalk region (yellow arrows) and *Cas⁻*, *Eya⁺* cells in the main body cell region (white arrowheads) in germaria expressing *hep[RNAi]* (J). (K) Quantification of frequency of germaria with tube-like and expanded stalk phenotype in ovarioles with mosaic or fully marked wild-type (WT) and *hep^{G0107}* mutant clones. Chi-squared test: **** = $p < 0.0001$, $n \geq 59$. (L) Quantification of the frequency of germaria with *Cas⁺*, *Eya⁺* in the stalk region in germaria with *hep[RNAi]* alone or *109-30^{ts}* driving expression of *hep[RNAi]*. Student's t-test: ** = $p < 0.01$, n.s. = not significant, $N = 3$ flies, $n \geq 86$ ovarioles.

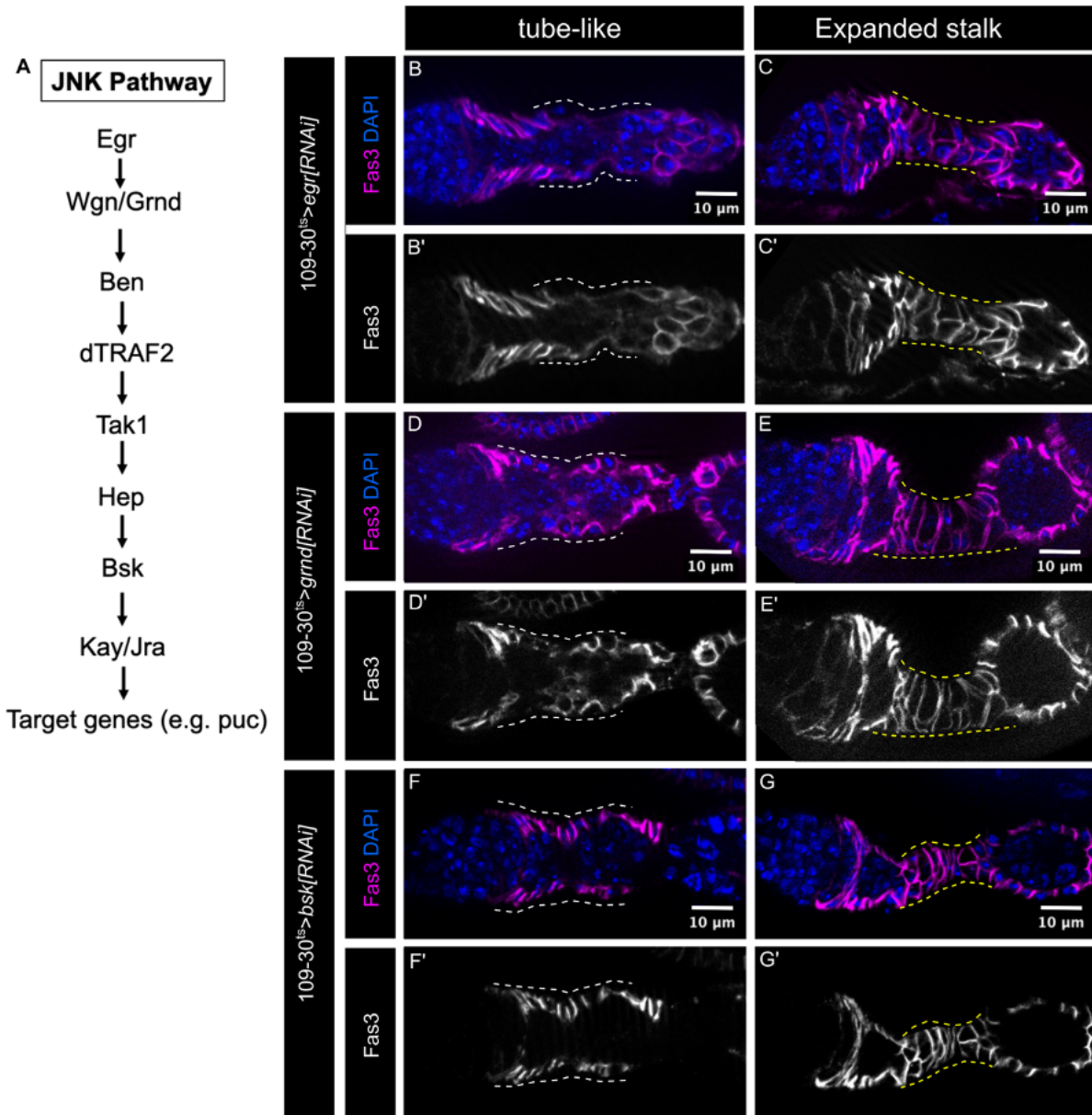


Figure 3.5. JNK signaling is required for follicle formation and stalk cell differentiation. (B-G) Ommatidia with *109-30^{ts}* driving RNAi against *egr*, *grnd*, or *bsk* stained for Fas3 (magenta), and DAPI (blue). Expanded stalk phenotypes (yellow dashed lines) and tube-like phenotypes (white dashed lines) are indicated.

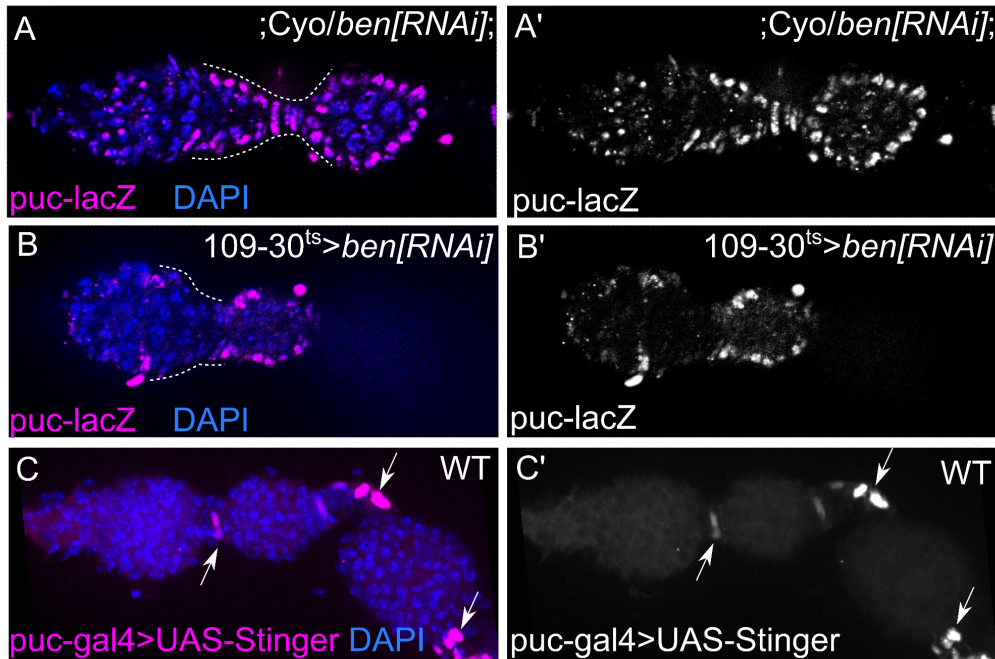


Figure 3.6. Expression pattern of additional reporters for JNK signaling. (A-B) JNK reporter, *puc-lacZ*, expressed in controls (*;CyO/ben[RNAi]*) and ovarioles with *109-30^{ts}* driving RNAi against *ben* stained for Fas3 (magenta) and DAPI (blue). (C) JNK reporter, *puc-gal4>UAS-Stinger*, expressed in control ovarioles.

Preliminary data collected using JNK-signaling reporters, *puc-lacZ* and *puc-gal4>UAS-Stinger*, indicated that JNK signaling is active in the FSC lineage, consistent with the AP-1 reporter pattern reported in the publication. Notably, the *puc-lacZ* expression pattern was broader than the expression pattern observed when using *puc-gal4>UAS-Stinger* and *AP-1-GFP*. Additional experiments to replicate the *puc-lacZ* preliminary findings would be useful, especially since phenotypic effects of the loss of JNK signaling have been characterized in pre-FCs, consistent with the expression pattern seen in Fig 3.6A-C.

Loss of JNK signaling impairs the activation of the Notch signaling reporter, *NRE-GFP*

Stalk cells are specified by JAK-STAT signaling from polar cells, and differentiation toward the polar cell fate is induced in early pFCs by Notch signaling (Assa-Kunik et al., 2007; Dai et al., 2017; Lopez-Schier and St Johnston, 2001). Therefore, we next investigated whether a loss of JNK signaling impairs JAK-STAT or Notch signaling in the FSC lineage. Consistent with previous results (Melamed and Kalderon, 2020; Vied et al., 2012), we found that the JAK-STAT reporter, *10x-STAT-GFP* (Bach et al., 2007), is active throughout the early FSC lineage in wild-type ovarioles. This pattern was unaffected in *ben^A* or *hep^{G0107}* clones, indicating that JNK signaling is not required for JAK-STAT signaling in the FSC lineage (Fig. 3.7).

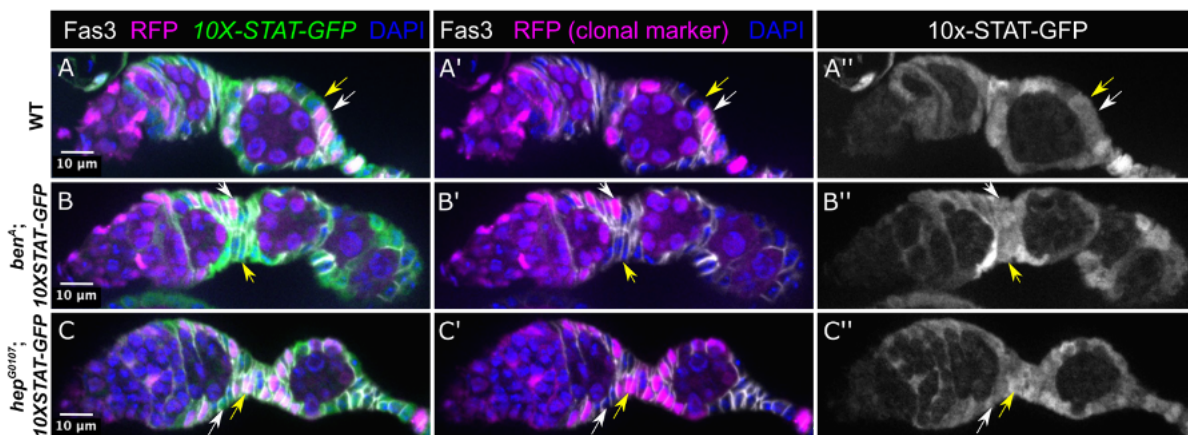


Figure 3.7. JNK signaling does not affect the pattern of JAK-STAT signaling in the FSC lineage.

(A-C) Ovarioles with *10x-STAT-GFP* and wildtype, *ben^A*, or *hep^{G0107}* RFP⁻ clones stained for RFP (magenta) GFP (green) Fas3 (white) and DAPI (blue). The pattern of GFP expression is similar in RFP⁻ (yellow arrows) and RFP⁺ (white arrows) cells.

The Notch pathway reporter, *NRE-GFP*, was detectable in wild-type ovarioles at the Region 2a/2b border where Notch signaling induces differentiation toward the polar cell fate, and again in mature polar cells starting in Region 3/Stage 1 follicles, as expected (Dai et al., 2017; Johnston et al., 2016). In contrast, the *NRE-GFP* signal was absent from the Region 2a/2b border and in mature polar cells in some germaria with *ben^A* or *hep^{G0107}* clones, suggesting that loss of JNK signaling impairs Notch pathway activation in

follicle cells (Fig. 3.8A-C). The cells in this region are closely packed together and only a subset normally expresses *NRE-GFP*. Thus, to simplify the comparison between genotypes, we focused on germaria in which all follicle cells in the germarium were marked by the lack of GFP, and thus part of a clone. In wild-type controls, 83.3% (n=12) of germaria had detectable *NRE-GFP* signal in Region 2b, whereas this frequency was significantly lower in germaria with *ben^A* (36.4%, n=22) or *hep^{G0107}* (0%, n=12) mutant clones (Fig. 3.8A-C, 3.8G). In addition, we found that the *NRE-GFP* signal was also frequently absent from mature polar cells, which can be identified as small clusters of cells with high levels of Fas3 staining, in *ben^A* or *hep^{G0107}* mutant clones compared to controls (Fig. 3.8D-F, 3.8H). However, since Notch signaling in Region 2b is required for the differentiation of pFCs into polar cells and we frequently observed polar cell clusters in *ben^A* and *hep^{G0107}* clones (Fig. 3.8D-F), the functional significance of the loss of *NRE-GFP* signal in pFCs is unclear.

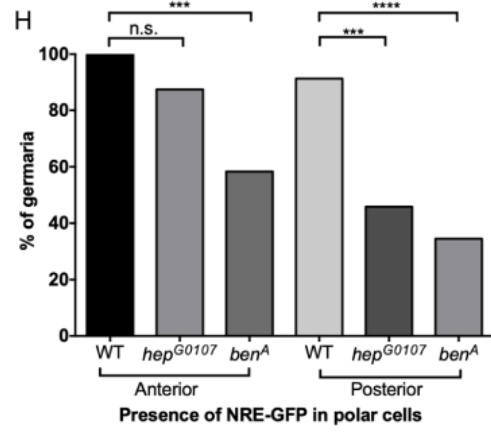
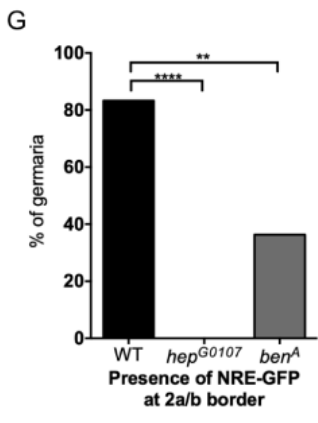
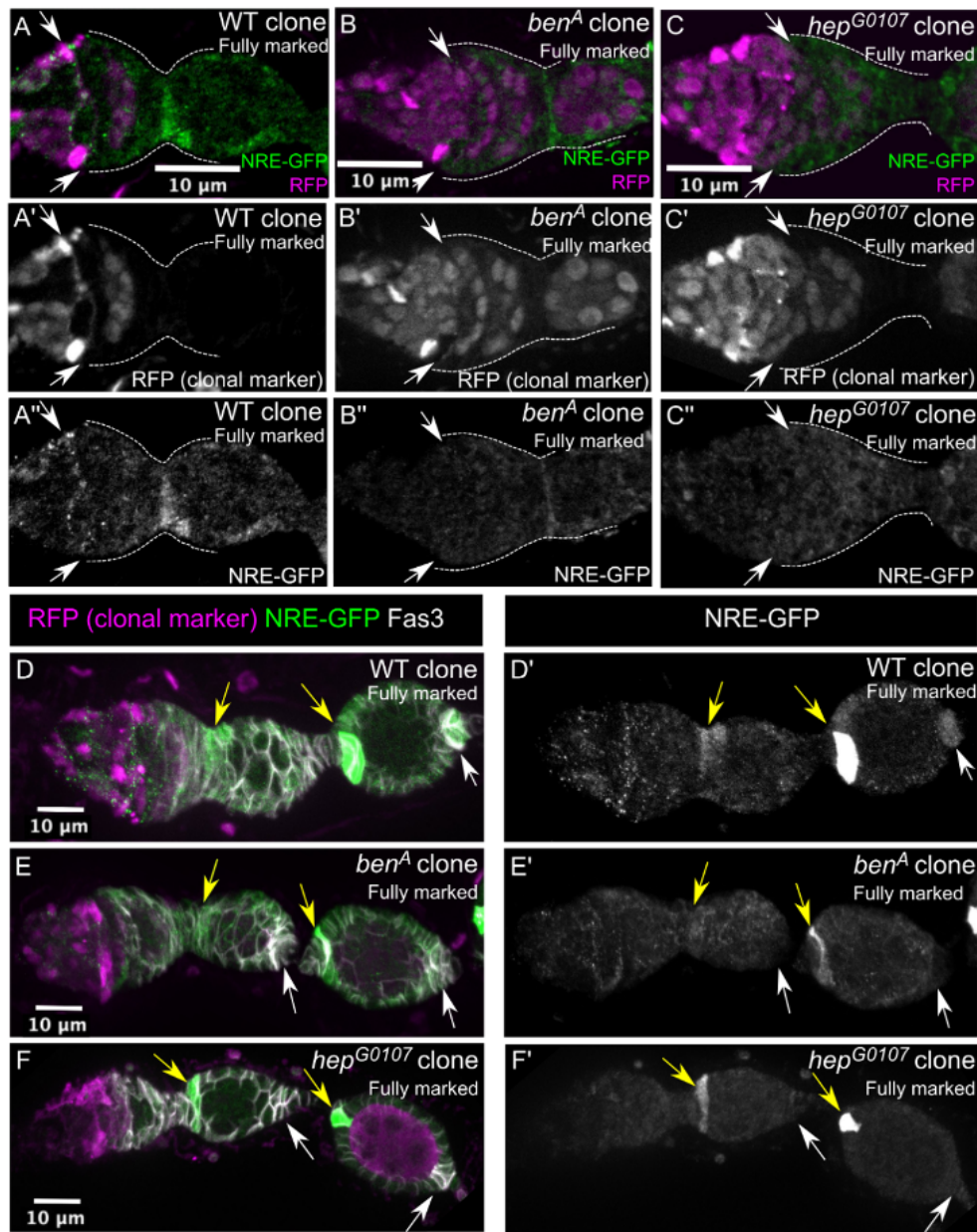


Figure 3.8. JNK signaling is required for the normal expression of the Notch signaling reporter, *NRE-GFP*.

(A-F) Ovarioles in which the follicle cell populations in the germarium and first two follicles are fully marked by the lack of RFP stained for GFP (green), RFP clonal label (magenta) and Fas3 (white). The RFP⁻ clones are either a wild-type control (WT) (A, D), *ben^A* (B, E), or *hep^{G0107}* (C, F). The germarium is outlined with white dashed lines in A-C, the Region 2a/2b border is indicated with white arrows in A-C, the anterior polar cell clusters are indicated with yellow arrows in D-F, and the posterior polar cell clusters are indicated with white arrows in D-F. (G-H) Quantifications of the frequencies of germaria with *NRE-GFP* expression at the 2a/b border (G) and *NRE-GFP* expression in anterior and posterior polar cell clusters (H) in germaria with WT, *hep^{G0107}* and *ben^A* mutant clones. The *NRE-GFP* signal is typically detectable in all three of these locations in the control ovarioles but is detectable in these locations at lower frequencies in *ben^A* or *hep^{G0107}* mutant ovarioles. Chi-squared test: **** = p<0.0001, *** = p<0.001, ** = p<0.01, n.s. = not significant, n≥12 ovarioles.

Impaired JNK signaling causes retention of phosphorylated ERK in pFCs, which blocks pFC differentiation

The transition from the FSC to pFC fate is characterized by an abrupt decrease in the level of double phosphorylated ERK (pERK), which is an indicator of EGFR signaling, and a gradual decrease in *Ptc-pelican-GFP*, which is a reporter of Hh signaling (Castanieto et al., 2014; Sahai-Hernandez and Nystul, 2013). To determine whether *ben* mutants affect the pattern of pERK, we first generated ovarioles with *ben^A* mutant clones or *ben[RNAi]* driven with either *109-30^{ts}* or the pFC driver, *stl-Gal4*, and stained for pERK. We found that pERK was clearly detectable in cells at the Region 2a/2b border, and then downregulated in Region 2b in the control ovarioles, as reported previously. In contrast, the pERK signal was strong in pFCs throughout Region 2b in ovarioles with either *ben^A* clones or with *ben[RNAi]* driven by *109-30^{ts}* or *stl-Gal4^{ts}* (Fig. 3.9A-E, 3.9J, 3.10A-B). We even observed a small but significant increase in the frequency of ovarioles with pERK⁺ pFCs in *ben^{A/+}* ovarioles (Fig. 3.9C, “unmarked” category). Likewise, RNAi knockdown of the JNK pathway components *egr*, *grnd*, *traf6* or *hep* driven by *109-30^{ts}* or *hep* driven by *stl-Gal4^{ts}* also caused retention of pERK in pFCs throughout Region 2b (Fig. 3.9D, F-J and Fig. 3.10C).

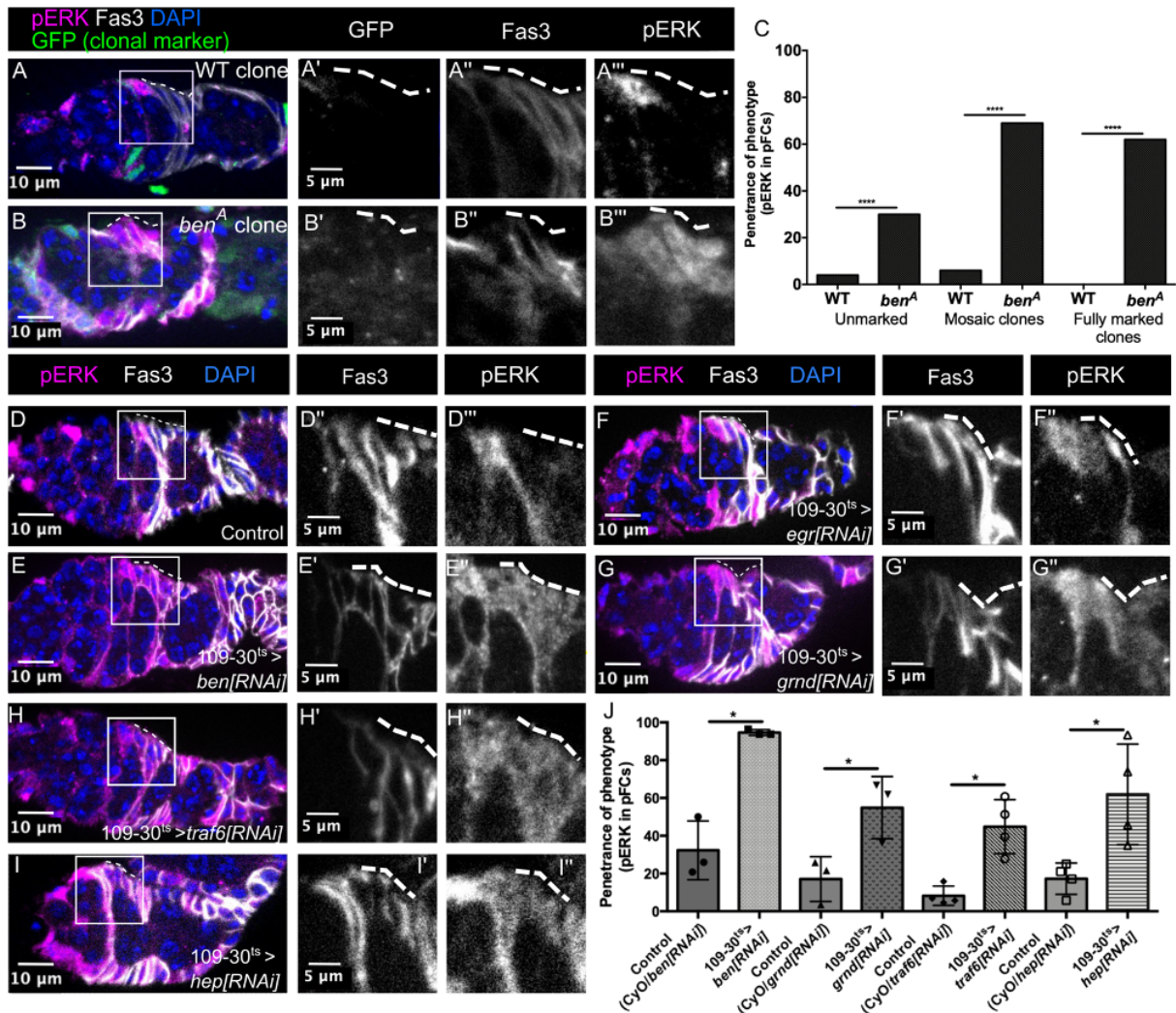


Figure 3.9. JNK signaling is required to decrease pERK in pFCs.

(A-B) Ovarioles with wild-type (WT) or *ben^A* GFP⁻ clones stained for GFP (green), pERK (magenta), Fas3 (white) and DAPI (blue). The pERK signal is absent in the pFCs within control clones (white dashed lines, A), but clearly detectable in pFCs within *ben^A* clones (white dashed lines, B). (C) Quantification of the frequency of ovarioles with pERK signal in pFCs in ovarioles that have all GFP⁺ (unmarked) follicle cells, a mosaic population of follicle cells, or all GFP⁻ follicle cells (fully marked). Chi-squared test: *** = $p < 0.001$, **** = $p < 0.0001$, $n \geq 20$ unmarked clones, $n \geq 42$ mosaic and $n \geq 20$ fully marked follicle cell lineage. (D-I) Ovarioles with *109-30^{ts}* alone (D) or *109-30^{ts}* driving expression of RNAi against *ben*, *egr*, *grnd*, *traf6*, or *hep* (E-I) stained for Fas3 (white), pERK (magenta) and DAPI (blue). The pERK signal is absent in pFCs in the control ovarioles (white dashed lines, D) but clearly detectable in the pFCs of the mutant ovarioles (white dashed lines, E-I). (J) Quantification of the frequency of germaria with the pERK signal in pFCs in the indicated genotypes and their paired controls (*109-30^{ts}* alone). Student's t-test: * = $p < 0.05$, n.s. = not significant, $N \geq 3$ flies, $n \geq 79$ ovarioles.

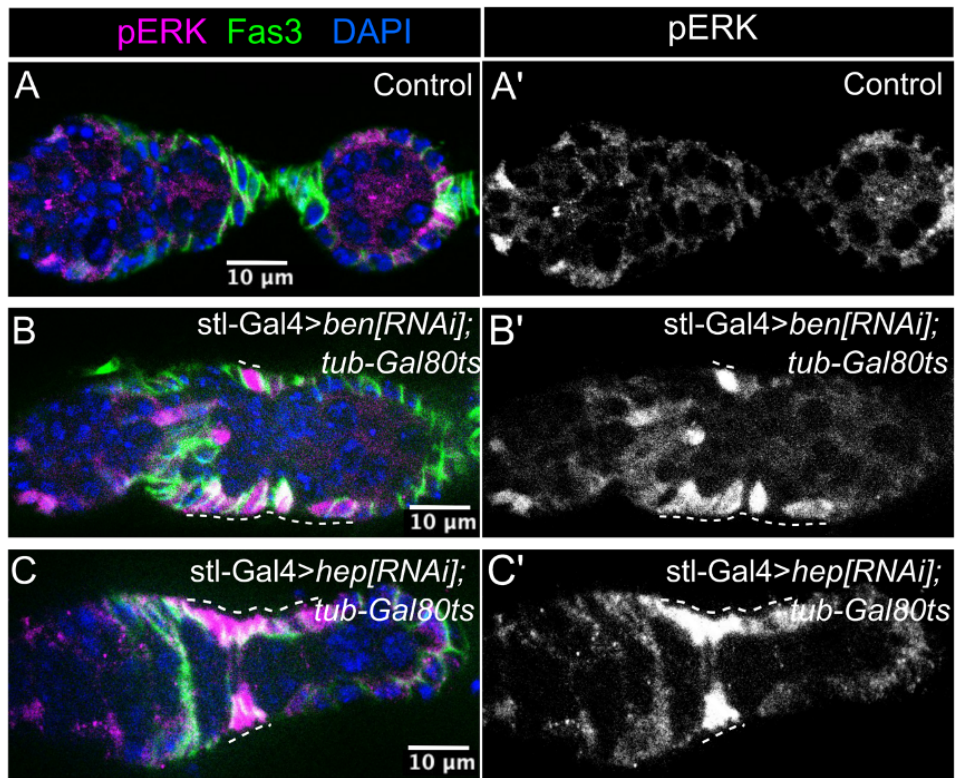


Figure 3.10. JNK signaling is required in pFCs to decrease pERK in pFCs.

(A-C) Ovarioles with *stl-Gal4* alone (A) or in combination with *UAS-ben[RNAi]* or *UAS-hep[RNAi]* to knockdown gene expression specifically during adulthood, stained for pERK (magenta), Fas3 (green) and DAPI (blue). The pERK signal is absent in pFCs in the control ovarioles (A) but clearly detectable in the pFCs of the mutant ovarioles (white dashed lines, B-C).

To determine whether other aspects of EGFR signaling are affected, we assayed for cell polarity defects in *ben^A* mutants. Constitutive activation of EGFR signaling interferes with the maturation of apical cell polarity in the early FSC lineage (Castanieto et al., 2014). However, we observed no defects in the localization of apical or lateral markers in *ben^A* pFCs (Fig. 3.11), indicating that, although loss of JNK signaling causes retention of pERK in pFCs, it does not phenocopy the impaired maturation of cell polarity that has been observed with constitutive EGFR signaling (Castanieto et al., 2014).

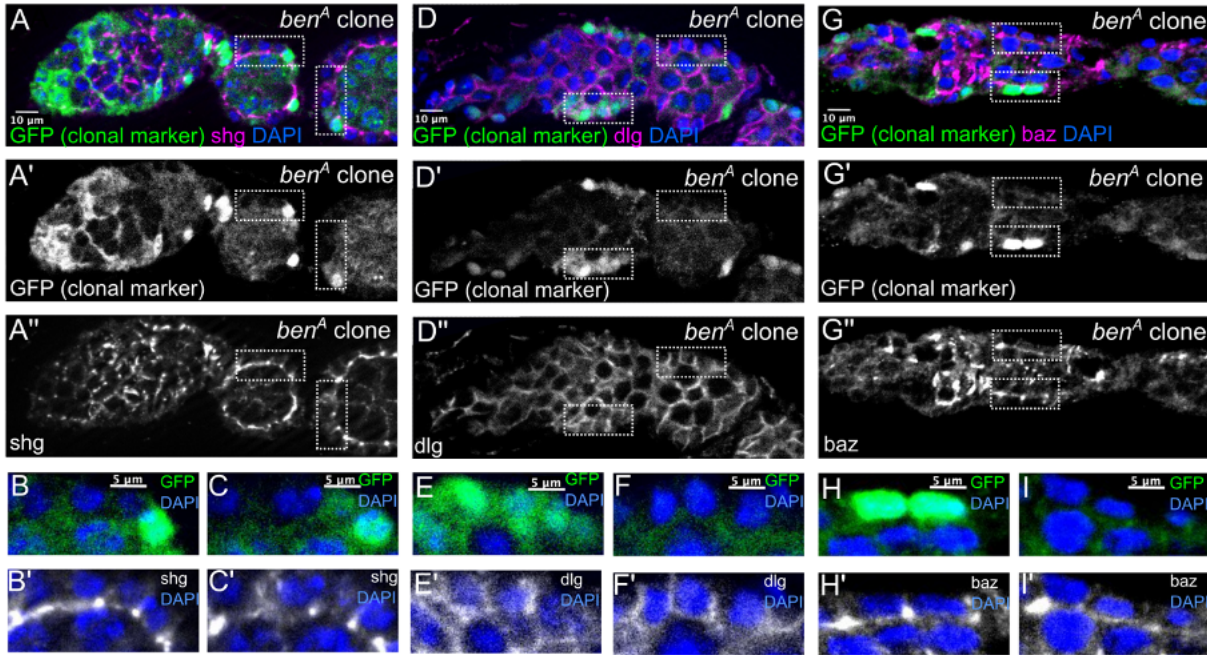


Figure 3.11. *ben^A* clones do not exhibit cell polarity defects.

(A-I) Ovarioles with *ben^A* GFP⁻ clones stained for GFP (green), DAPI (blue) and either Shg (A-C), Dlg (D-F), or Baz (G-I) in magenta (A, D, and G) or white (B, C, E, F, H and I). The GFP and cell polarity marker channels are separated out in A'-A'', D'-D'', and G'-G''. The regions bounded by the rectangular boxes in A, D and G are magnified in B-C, E-F, and H-I (and also rotated in C). There are no detectable differences in the localization of cell polarity markers between GFP⁺ and GFP⁻ cells, as can be seen in these magnified regions.

To explore whether activation of ERK affects pFCs differentiation, we overexpressed a constitutively active allele, *ERK^{SEM}*, in the early FSC lineage during adulthood with *109-30^{ts}* and stained for Fas3, Cas, and Eya. Indeed, upon overexpression of *ERK^{SEM}*, we observed a significant increase in ovarioles with an expanded stalk, a tube-like phenotype, or both, compared to controls (Fig. 3.12A-C, F, 56.3%, n≥114). In addition, we found Cas⁺, Eya⁺ cells within the stalk region in a majority of mutant ovarioles (Fig. 3.12D-E, G, 75.8% ± 25.0%, n≥88). As with knockdown of JNK pathway components, the cells in the main body cell region were Cas⁻, Eya⁺. These observations indicate that increased ERK activity in pFCs impairs differentiation toward the stalk cell fate and suggest that the aberrant activation of ERK

contributes to the pFC differentiation defects we observed in ovarioles with impaired JNK signaling in the early follicle cell lineage.

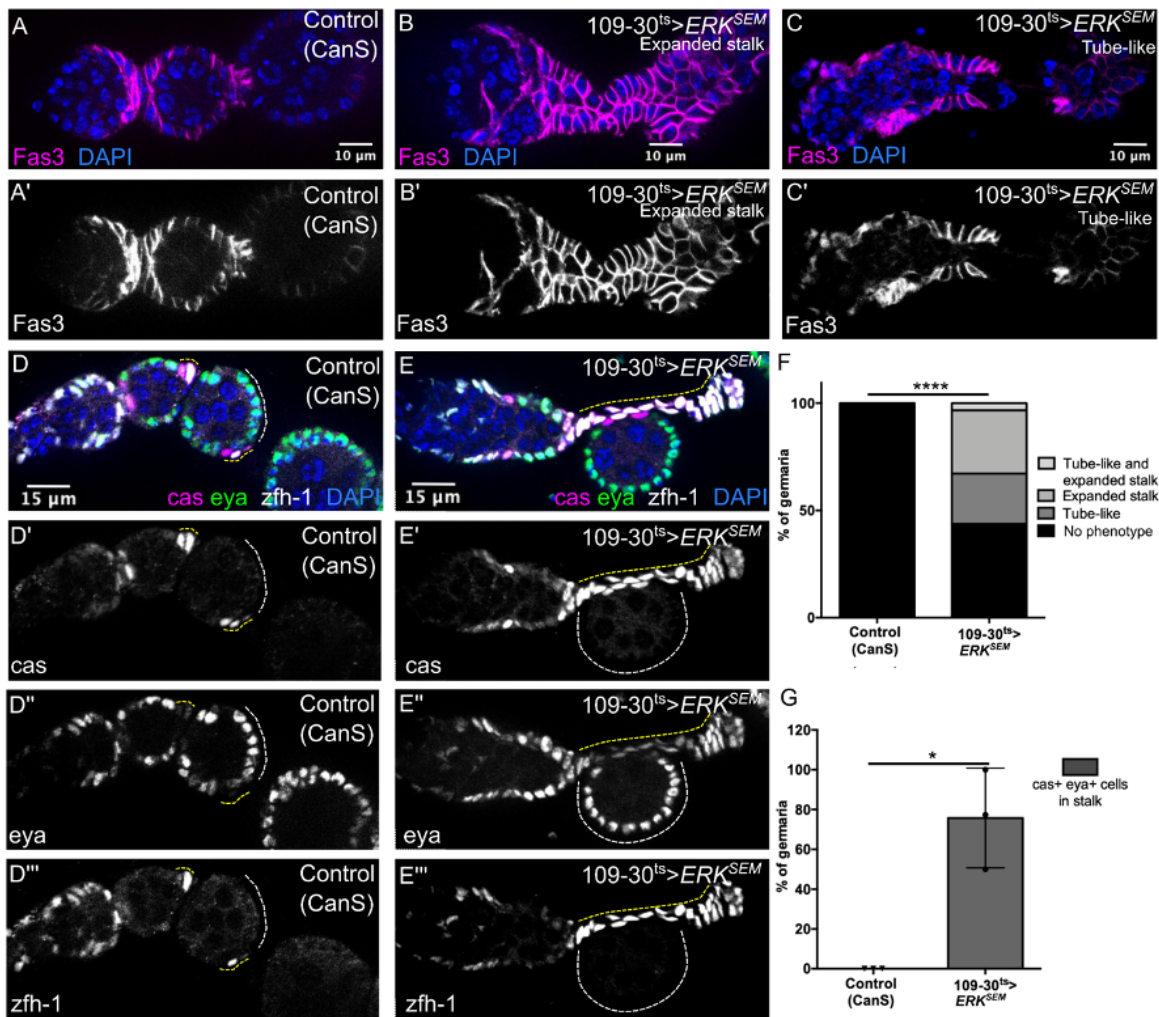


Figure 3.12. Constitutively active *ERK* in the FC lineage causes defects in stalk formation and differentiation.

(A-E) Ovarioles from the Canton-S (CanS) wild-type strain (A) or with *109-30^{ts}* driving expression of *ERK^{SEM}*, a constitutively active allele of *ERK*, (B-C) stained for Fas3 (magenta) and DAPI (blue) in panels A-C or Cas (magenta), Eya (green), Zfh-1 (white) and DAPI (blue) in panels D-E. Overexpression of *ERK^{SEM}* causes expanded stalk phenotypes (B), tube-like phenotypes (C), and Cas⁺, Eya⁺ cells in the stalk region (yellow dotted lines in E) but does not prevent the formation of Cas⁻, Eya⁺ cells in the main body cell region (white dotted lines in E). The expression pattern of *zfh-1* remained unaffected (D''', E'''). Progeny were maintained at 18°C until eclosion, and then shifted to 29°C for 18 days. (F-G) Quantifications of the frequency of germaria with an expanded stalk or tube-like phenotype (F) or with Cas⁺, Eya⁺ cells in

the stalk region (G). Chi-squared test: **** = $p < 0.0001$, n.s. = not significant, $n \geq 114$ (F) and Student's t-test: * = $p < 0.0001$, $N = 3$ flies, $n \geq 88$ ovarioles (G).

pERK is a reporter for EGFR signaling and a marker for FSCs, which gets downregulated in pFCs. Since we observed an effect on pERK retention in pFCs, we asked whether there were additional markers of FSC state that failed to be downregulated in *ben* mutant conditions. Single cell sequencing of the FSC lineage revealed that Bin and Wnt4 are FSC markers that are downregulated in pFCs. When we stained ovarioles in which *ben[RNAi]* or *hep[RNAi]* have been driven by *109-30^{ts}* and compared them with wild-type, we qualitatively noted that there seemed to be an increased number of pFCs posterior to the 2a/b border that express FSC marker Bin when *ben[RNAi]* or *hep[RNAi]* is driven using *109-30^{ts}* (Fig. 3.13). Further experiments will be necessary to replicate and quantify these effects. In contrast, the expression pattern of Wnt4 was not significantly different between JNK mutant and WT conditions, suggesting that all markers associated with FSC state might not be abnormal in JNK mutant pFCs (Fig. 3.14).

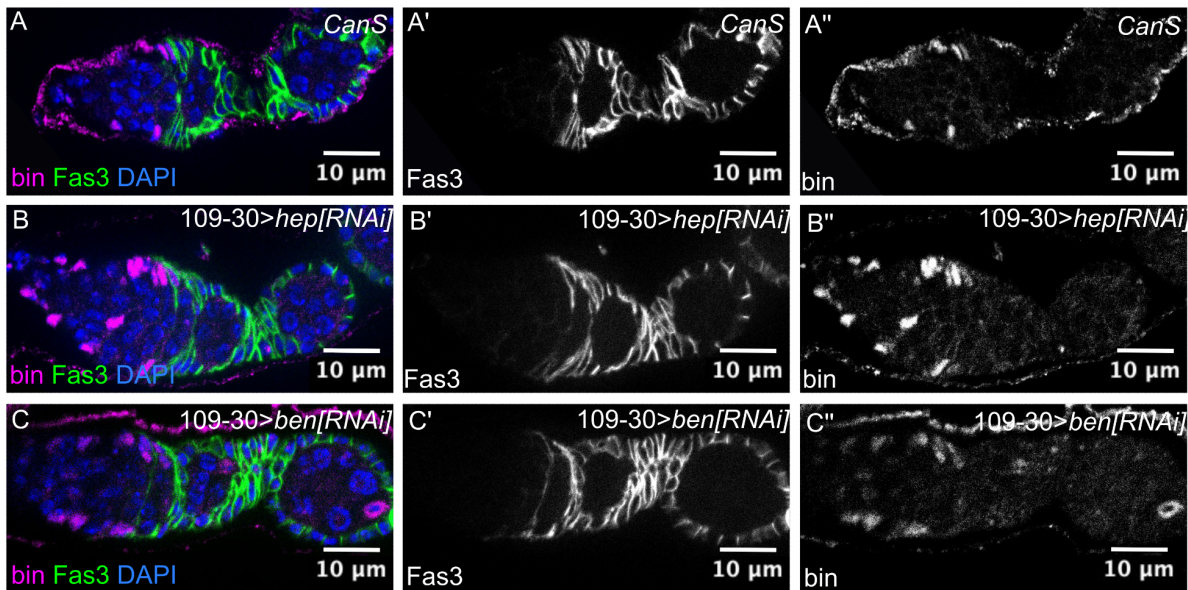


Figure 3.13. JNK pathway promotes FSC marker expression, Bin, in pFCs

(A-C) Ovarioles from the Canton-S (CanS) wild-type strain (A) or with *109-30^{ts}* driving expression of *hep[RNAi]* (B) or *ben[RNAi]* (C) stained for Bin (magenta), Fas3 (green) and DAPI (blue).

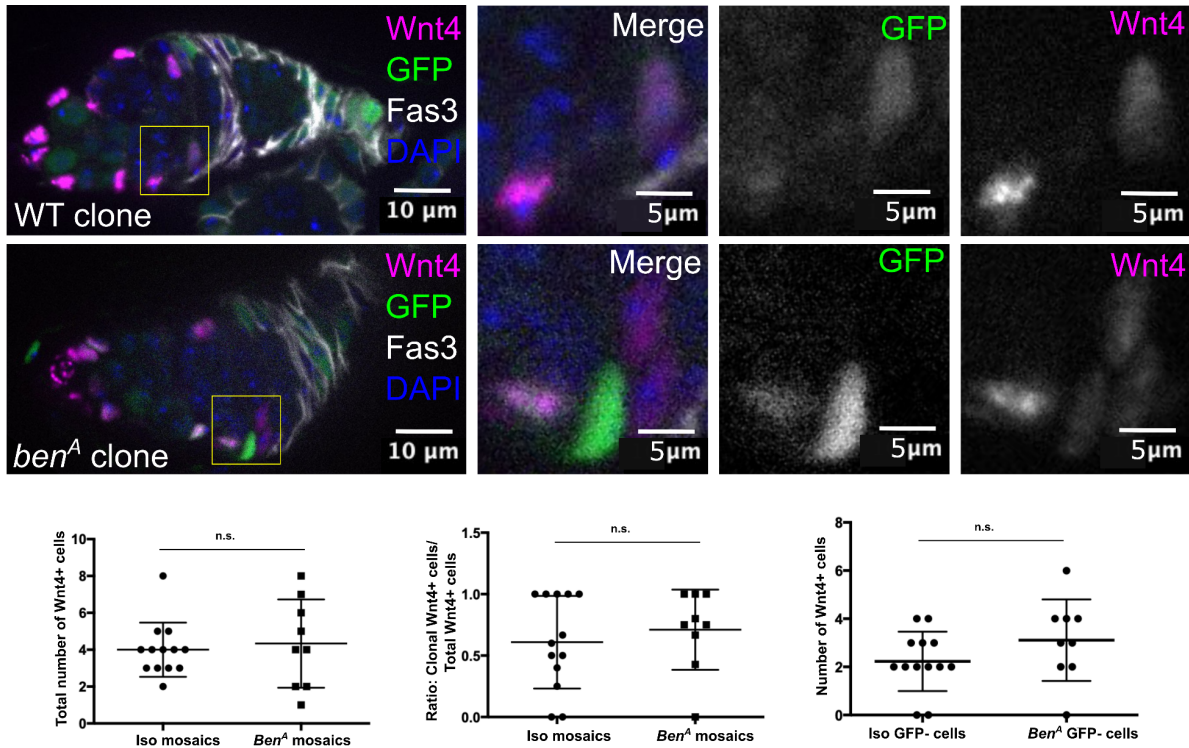


Figure 3.14. Ben does not affect FSC marker, Wnt4, expression in FSCs

Ovarioles containing wild-type clones or *ben^A* mutant clones stained for Wnt4 (magenta), Fas3 (white) and GFP (clonal marker, green). Quantification of cells expressing Wnt4 posterior to the 2a/b border.

Ben functions in a JNK pathway independent manner to promote Hh signaling in FCs

Next, we assayed for *Ptc-pelican-GFP* expression in wild-type and mutant tissue. In wild-type ovarioles, we observed a progressive decrease of *Ptc-pelican-GFP* expression throughout Region 2b (Fig. 15A), as expected (Sahai-Hernandez and Nystul, 2013; Ulmschneider et al., 2016). In contrast, the *Ptc-pelican-GFP* signal was significantly higher in *ben^A* cells throughout Region 2b, and remained clearly detectable in follicle cells throughout the germarium (Fig. 15B, D, E). However, we did not observe a significant increase in *Ptc-pelican-GFP* signal in *hep^{G0107}* cells throughout Region 2b (Fig. 15C, F). To further explore the effect of Hh signaling, we assayed for *zfh-1* expression, which is known to be expressed in ovarian somatic cells and is a direct target of Hh signaling in the *Drosophila* testis (Michel et al., 2012). In wild-type germaria, *zfh-1* is consistently expressed in escort cells, FSCs, pFCs in Region 2b, and stalk cells, and tapers off in the pFCs in Region 3 (Fig. 15G). Specifically, only $62.9\% \pm 16.8$ of germaria have *Zfh-1⁺* pFCs in

Region 3, and *zfh-1* expression is completely absent in the main body follicle cells of the first budded follicle downstream from the germarium (referred to as a Stage 2 follicle). Overexpression of *Hh* driven with *109-30^{ts}*, induced the expression of *zfh-1* in follicle cells throughout Region 3 and Stage 2 follicles, indicating that, as in the testis, *zfh-1* expression is activated by Hh signaling in the follicle epithelium (Fig. 3.15H). In ovarioles with RNAi knockdown of *ben*, we observed a significant increase in the number of germaria with *Zfh-1*⁺ follicle cells in Region 3 and Stage 2 follicles (Fig. 3.15I and Fig. 3.15K). In contrast, RNAi knockdown of *hep* driven by *109-30^{ts}* had no effect on the pattern of *Ptc-pelican-GFP* or *zfh-1* expression (Fig. 3.15J and Fig. 3.15L). These observations indicate that Ben functions in a JNK pathway independent manner to shape the patterning of Hh signaling in pFCs and main body follicle cells of newly budded follicles.

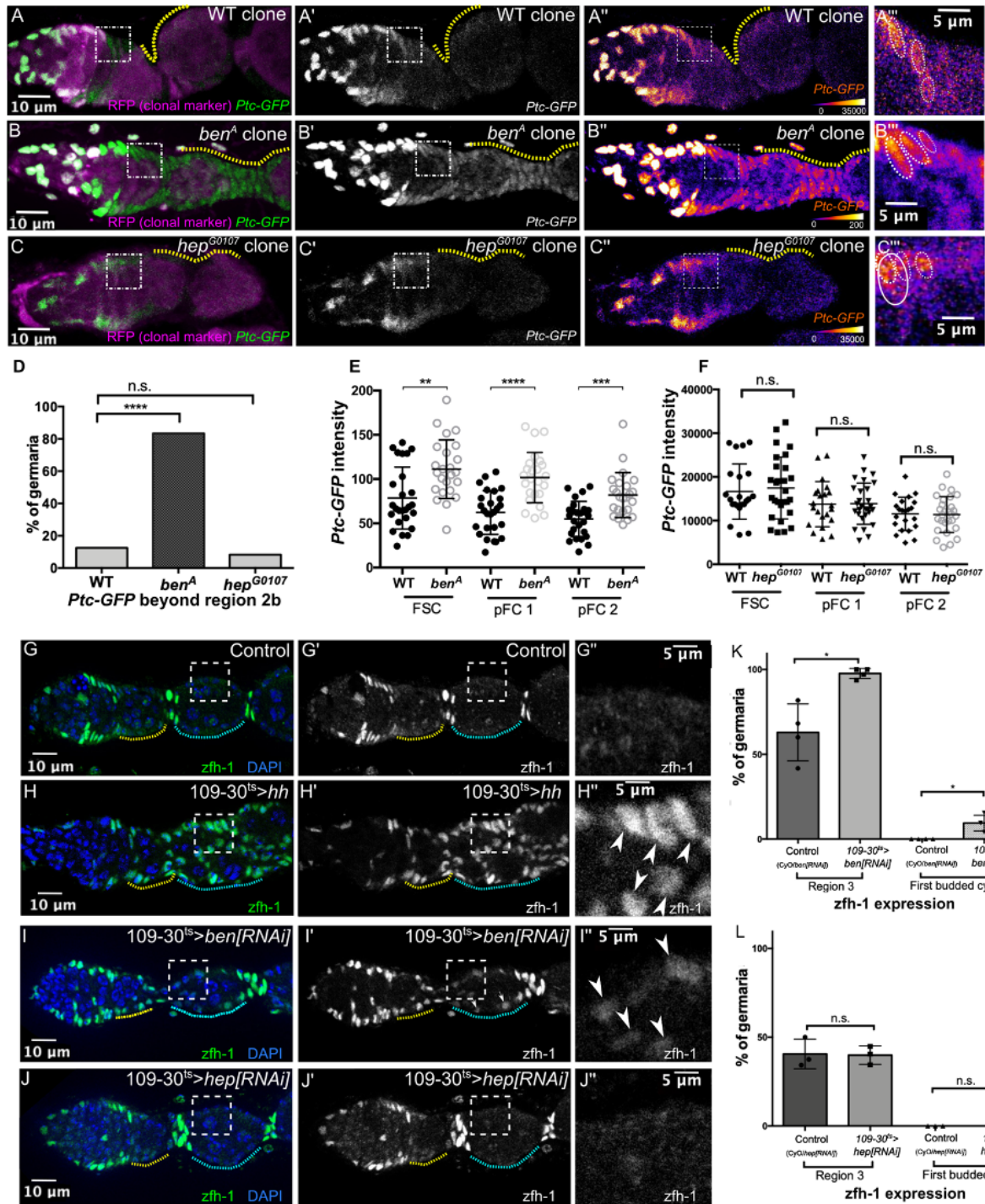


Figure 3.15. Ben is required for proper patterning of Hh signaling in the early FSC lineage.

(A-C) Ovariolar clones with *Ptc-pelican-GFP* and wild-type (WT), *hep^{G0107}*, or *ben^A* RFP⁻ clones stained for RFP (magenta) and GFP (green). The *Ptc-pelican-GFP* channel is shown with colorimetric scale in A''-C'' to highlight differences in intensity. Measurements of the *Ptc-pelican-GFP* signal were taken from the FSC, identified as the anterior-most cell in the clone, and next two pFCs downstream from the FSC (white dotted

lines in the insets). (D-F) Quantifications showing percent of germaria with *Ptc-pelican-GFP* expressed beyond Region 2b (D), and *Ptc-pelican-GFP* intensity in FSCs and early pFCs (E-F) within clones of each genotype. Chi-squared test, n.s. = not significant, ** = $p < 0.01$, *** = $p < 0.001$, **** = $p < 0.0001$, $n \geq 12$ ovarioles. (G-J) Ovarioles with *ben[RNAi]* or *hep[RNAi]* without *109-30^{ts}* (Control, G) or *109-30^{ts}* driving expression of *Hh* (H), *ben[RNAi]* (I), or *hep[RNAi]* (J), stained for Zfh-1 (green) and DAPI (blue). Region 3 marked with yellow dotted lines and Stage 2 marked with cyan dotted lines. The insets show the aberrant expression of *zfh-1* in main body cells of Stage 2 follicles upon overexpression of *Hh* or RNAi knockdown of *ben*, but not RNAi knockdown of *hep*. (K-L) Quantifications of the frequency of ovarioles in which *zfh-1* is expressed in follicle cells in Region 3 and Stage 2 follicles in the indicated genotypes. Student's t-test, * = $p < 0.05$, n.s. = not significant, $N \geq 3$ flies, $n \geq 66$ ovarioles.

Loss of Ben increases proliferation in pFCs

Hedgehog signaling regulates proliferation in the early FSC lineage (Hartman et al., 2010; Hartman et al., 2013; Huang and Kalderon, 2014; Singh et al., 2018; Zhang and Kalderon, 2000), so our finding that *ben* mutants have increased Hh signaling raised the possibility that the rate of proliferation may also be increased. To test this possibility, we used EdU assays, which identify cells in S-phase, in ovaries with wild-type, *hep^{G0107}*, or *ben^A GFP⁻* clones. In wild-type mosaic ovarioles, we found no significant difference in the percentages of EdU⁺ cells (i.e. the “proliferation indices”) in the GFP⁻ and GFP⁺ populations, as expected. Consistent with our finding that *hep^{G0107}* mutant pFCs do not have increased levels of Hh signaling, we observed no significant difference in the proliferation indices of *hep^{G0107}* homozygous mutant follicle cells compared to *hep^{G0107}/+* heterozygous cells. By contrast, in mosaic ovarioles with *ben^A* clones, we observed a significantly higher proliferation index in the GFP⁻ (*ben^A/ben^A*) population compared to the GFP⁺ (*ben^A/+*) population (Fig. 3.16A-D). Likewise, we observed a significant increase in the EdU proliferation index in ovarioles that are fully marked *ben^A* follicle cell clones compared to ovarioles that are fully marked with wild-type control clones (Fig. 3.16E-G). Consistent with these results, we also observed a significantly higher frequency of cells that are positive for the M-phase marker, phosphohistone H3 (pH3) in fully marked ovarioles with *ben^A* clones compared to those with wild-type clones (Fig. 3.16H-K).

To confirm that the increased proliferation is due to a reduction of Ben but not Hep function, we also compared the proliferation indices of the follicle cell populations in germaria with *ben[RNAi]* or *hep[RNAi]* driven by *109-30^{ts}* to wild-type. Again, compared to the wild-type control, we observed a

significant increase in proliferation indices in germlaria with *ben[RNAi]*, but not *hep[RNAi]* (Fig. 3.16L). Taken together, these observations suggest that Ben has at least two distinct functions in the regulation of pFC differentiation: a JNK pathway dependent role in the regulation of pFC differentiation through the downregulation of pERK and possibly also increased receptivity to Notch signaling, and a JNK pathway independent role in the regulation of Hh signaling and proliferation within the early FSC lineage.

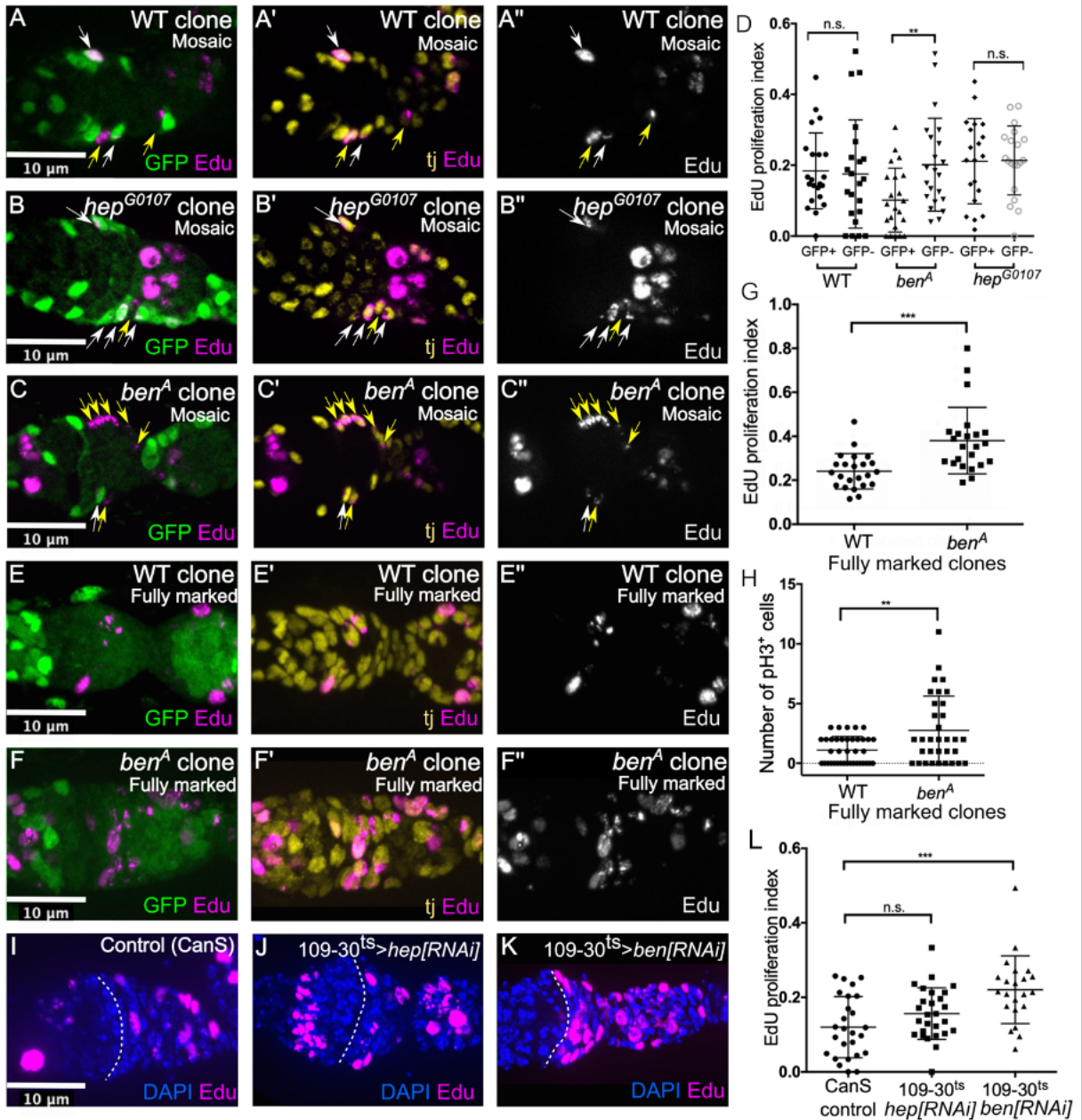


Figure 3.16. Loss of *ben*, but not *hep* causes increased proliferation in pFCs.

(A-C) Mosaic ovarioles with wild-type, *hep^{G0107}*, or *ben^A* clones stained for EdU incorporation (magenta) to identify cells in S-phase, the GFP clonal label (green), and Tj (yellow). Mosaic ovarioles contain both GFP⁺ (white arrows) and GFP⁻ (yellow arrows) cells. (D) Quantification of the EdU proliferation index in GFP⁺ and GFP⁻ cells in mosaic ovarioles of the indicated genotypes. Student's t-test, ** = $p < 0.01$, $n \geq 20$ ovarioles. (E-F) Ovarioles in which the follicle cell populations in the germarium are fully marked by the lack of GFP were stained for EdU incorporation (magenta), the GFP clonal label (green), and Tj (yellow). (G-H) Quantification of the EdU proliferation index (G) and the number of pH3⁺ follicle cells in germaria with fully marked wild-type or *ben^A* follicle cell populations (H). Student's t-test, ** = $p < 0.01$, *** =

p<0.001, n≥23 ovarioles. (I-K) Maximum intensity projection of ovarioles from Canton-S (CanS) flies (I) or *109-30^{ts}* driving *hep[RNAi]* or *ben[RNAi]* (J-K) stained for EdU incorporation (magenta) and DAPI (blue). (L) Quantification of the EdU proliferation index in the indicated genotypes. Student's t-test, *** = p<0.001, n.s. = not significant, n≥22 ovarioles.

E2 Ubiquitin ligase Bendless has been known to interact with several E3s and accessory proteins including Traf6, Dredd and Nopo. While Traf6, a core component of the JNK signaling pathway phenocopied the JNK-dependent differentiation defects first seen in *ben* mutants, the E3 ubiquitin ligase that Ben interacts with to affect Hh signaling had not been identified. We hypothesized that the E3 ubiquitin ligase responsible for *ben* mediated effects on Hh signaling, might also undergo increased proliferation in pFCs, phenocopying the *ben* mutant proliferation phenotype. *109-30^{ts}* drove the expression of *traff[RNAi]*, *dredd[RNAi]* and *nopo[RNAi]* (Fig. 3.17). Differentiation defects observed in these conditions included tube-like and epithelial gap phenotypes, similar to phenotypes observed in *ben* mutant conditions. Interestingly, preliminary evidence suggests that the number of Edu+ cells increased in ovarioles with *109-30^{ts}* expressing *dredd[RNAi]* (Fig. 3.17). Dredd is an accessory protein known to interact with Bendless, and a core component of the IMD pathway. Using *atta-GFP*, we examined the activity of IMD signaling in the FSC lineage, but could not identify any signal throughout the lineage. But, if these findings successfully replicate, it could be interesting to investigate whether Ben interacts with Dredd in the FSC lineage, and explore the mechanistic and functional consequences of the interaction.

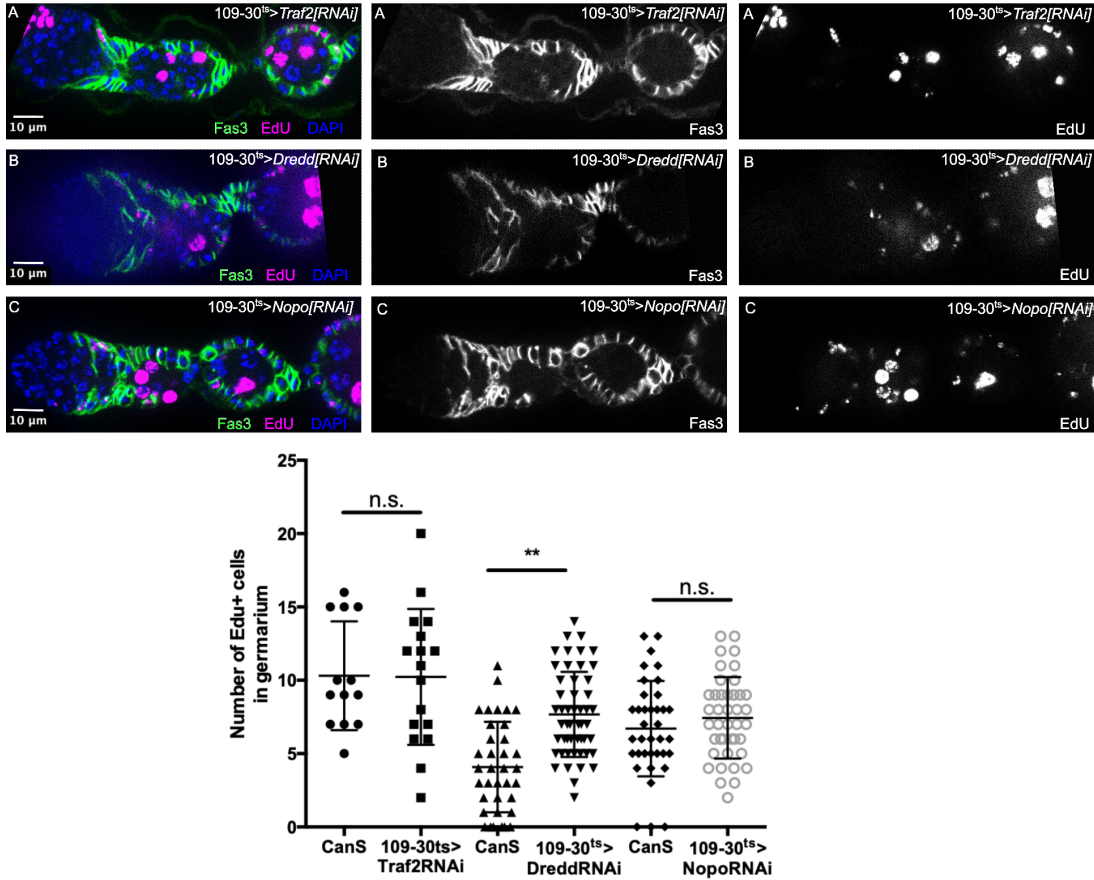


Figure 3.17. Morphological phenotypes and proliferation of FCs in ovarioles with RNAi knockdown against E3 ligases and accessory proteins that interact with Bendless.

(A-C) Ovarioles with *109-30^{ts}* driving expression of *traf[RNAi]*, *dredd[RNAi]* and *nopo[RNAi]* stained with Fas3 (green), EdU (magenta) and DAPI (blue). Graph depicts the quantification of the number of Edu+ cells in germaria in all conditions.

Loss of Ben causes hypercompetition in the FSC niche by regulating pFC proliferation and differentiation

Previous studies have shown that FSCs can be lost and replaced by cells from a neighboring FSC lineage (Kronen et al., 2014; Nystul and Spradling, 2007; Wang et al., 2012). In these studies, FSC clones are generated with a lineage tracing system that marks the FSCs and their progeny with a genetically heritable label, such as the lack of GFP (in a negatively-marked system, diagrammed in Fig. 3.18A) or the

expression of GFP (in a positively-marked system) (Fox et al., 2008; Hafezi and Nystul, 2001). When the lineage tracing system is used to label FSCs in an otherwise wild-type tissue, the marked and unmarked cells are functionally equivalent, and the pattern of FSC loss and replacement conforms to a model of neutral competition for niche occupancy (Clayton et al., 2007; Klein and Simons, 2011; Kronen et al., 2014). If the lineage tracing system simultaneously marks the cells and introduces a genetic mutation, the effect of the mutation on FSC niche competition can be tested by quantifying the changes in the frequencies of ovarioles with either a unmarked (i.e. unrecombined), mosaic, or fully marked (i.e. recombined) population of follicle cells in the germarium over time.

To confirm the hypercompetition phenotype of *ben^A*, we heat shocked flies to induce wild-type control or *ben^A* mutant clones that are marked by the lack of GFP in adult flies, and quantified the proportion of germaria with fully GFP⁻, mosaic, or fully GFP⁺ follicle cell populations at 6, 12 and 18 days post heat shock (dphs) (Fig. 3.18B-D). We observed a significant increase in germaria with *ben^A* mutant clones compared to wild-type, indicating that *ben^A* mutant cells are hypercompetitive for the FSC niche (Fig. 3.18E), consistent with our previous results (Cook et al., 2017). Additionally, we found that FSCs mutant for *ben^B*, an allele of *ben* that contains a missense point mutation, also displayed FSC hypercompetition, tube-like morphological phenotypes and increased pERK in pFCs (Fig. 3.18E and Fig. 3.19). In contrast, the frequency of germaria with *hep^{G0107}* clones was not significantly different from the control, indicating that downregulation of JNK signaling does not affect FSC niche competition (Fig. 3.18E). To confirm this result, we replicated experiments with another JNK pathway component, *traf6*, and found that loss of *traf6* resulted in no significant increase in FC proliferation and neutral FSC competition (Fig. 3.20). To confirm previous findings that increased proliferation alone is sufficient to explain FSC hypercompetition, we increased proliferation in FCs by overexpressing Cyclin E and String (CycE-Stg) and consistent with our expectations, it resulted in a significant increase in the frequency of germaria containing mutant clones overexpressing CycE-Stg compared to controls at every timepoint (Fig. 3.21). While the trend observed

suggests that overexpression of CycE-Stg causes FSC hypercompetition, future experiments are necessary to confirm that overproliferation alone using CycE-Stg results in a significant hypercompetitive bias.

To test whether the increased proliferation or increased Hh signaling that we observed in *ben^A* mutant clones is necessary for the hypercompetition phenotype, we used the GFP⁺ clonal marking system, MARCM (Lee and Luo, 2001) (Fig. 3.18F-I), to combine homozygosity for *ben^A* with expression of either *dap*, which slows the cell cycle by inhibiting cyclin dependent kinases (Lane et al., 1996), or *smo[RNAi]*. Indeed, we observed a significant reduction in clones expressing *dap* or *smo[RNAi]* either alone or in combination with *ben^A* compared to the control (Fig. 3.18I). Overexpression of *dap* or RNAi knockdown of *smo* in *ben^A* clones completely reversed the hypercompetition phenotype of *ben^A* mutant clones, causing them to become hypocompetitive. Moreover, we confirmed that RNAi knockdown of *smo* significantly reduces the rate of proliferation in pFCs (Fig. 3.18J), as measured by EdU incorporation (Huang and Kalderon, 2014). Collectively, these results indicate that the hypercompetition phenotype of *ben^A* mutants is not due to the differentiation defects caused by abnormal JNK signaling and suggest instead that it is due to the increased rate of proliferation induced by elevated Hh signaling in these mutants.

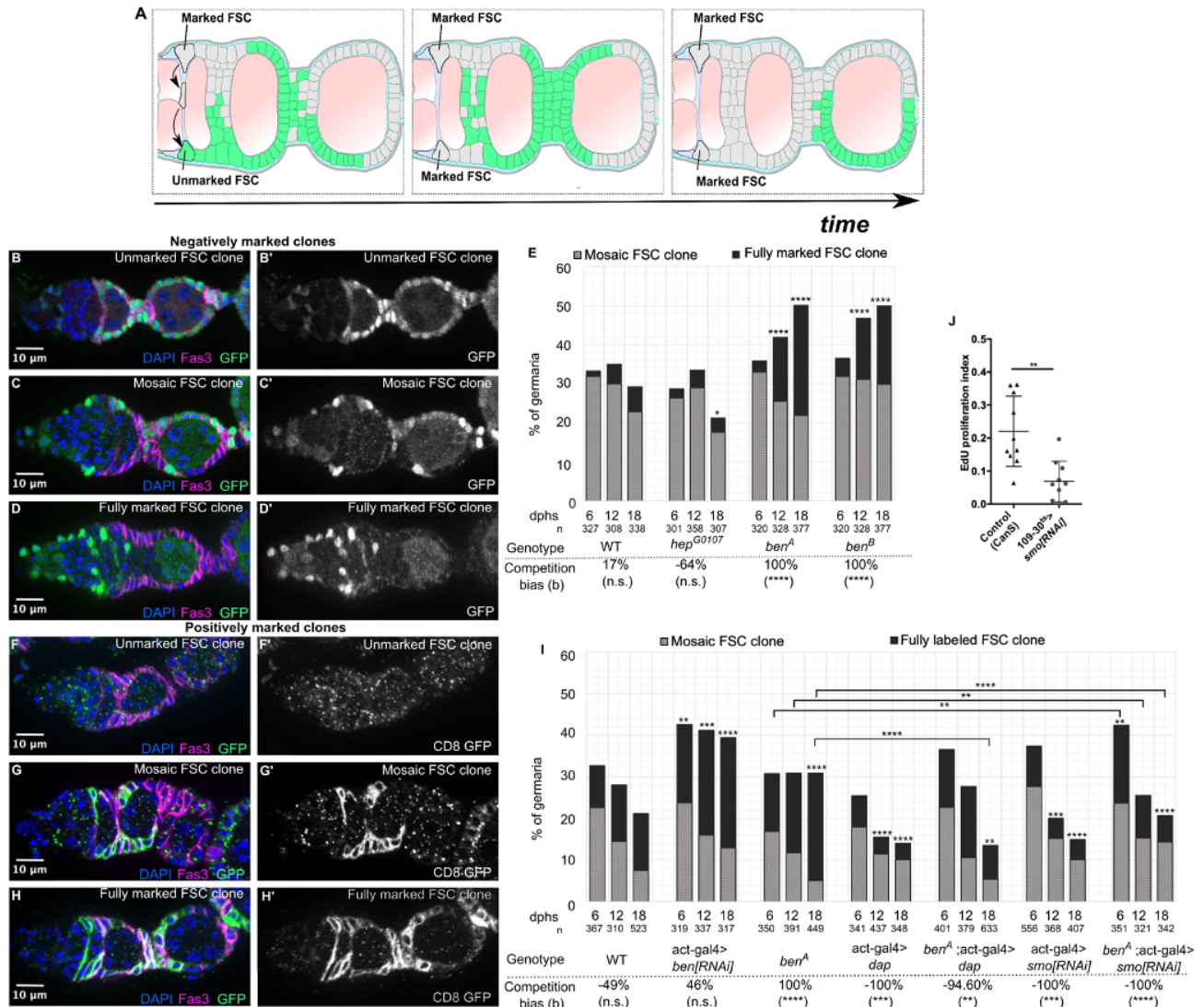


Figure 3.18. Hypercompetition in *ben* mutant clones is suppressed by inhibition of proliferation or Hh signaling.

(A) Schematic representation of FSC replacement through niche competition. (B-D) Ovarioles that either lack GFP⁻ clones (fully unmarked, B), contain both GFP⁺ and GFP⁻ follicle cells and thus are mosaic (C) or contain a follicle cell population that is fully GFP⁻ (fully marked, D) stained for GFP (green), Fas3 (magenta) and DAPI (blue). (E) Quantification of ovarioles with a mosaic or fully-marked clone pattern at 6, 12, and 18 days post heat shock (dphs) of the indicated genotypes. (F-H) Ovarioles with follicle cell populations that are unmarked (F), mosaic (G) and fully marked (H) with the GFP⁺-marked clonal marking system, MARCM, stained for GFP (green), Fas3 (magenta), and DAPI (blue). (I) Quantification of ovarioles with a mosaic or fully-marked clone pattern at 6, 12, and 18 days post heat shock (dphs) of the indicated genotypes. (J) Quantification of EdU proliferation index in ovarioles from Canton-S (CanS) flies or with *109-30^{ts}* driving expression of *smo[RNAi]*. Student's t-test, ** = $p < 0.01$, $n = 10$ ovarioles. In panels E and I, the competition bias (*b*) for the indicated genotypes, significance values for *b*, and the number of germaria scored (*n*) are shown below the graphs in E and I. Asterisks (*) above bar graphs indicate significance of results when compared to WT control ovarioles. Non-significant (n.s.) test statistics

between conditions are not shown. Chi-squared test, * = $p < 0.05$, ** = $p < 0.01$, *** = $p < 0.001$, **** = $p < 0.0001$.

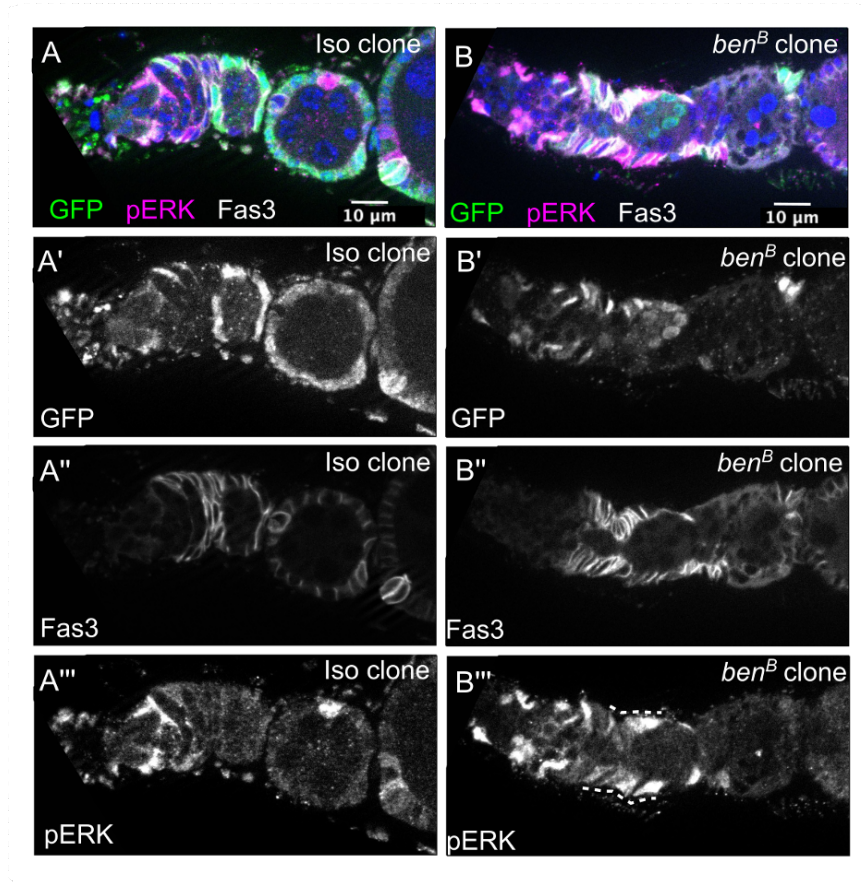


Figure 3.19: Ovarioles with *ben^B* clones exhibit expanded pERK and tube-like phenotypes. (A-B) Ovarioles with wildtype or *ben^B* GFP⁻ clones stained for GFP (green), pERK (magenta), Fas3 (white), and DAPI (blue). The presence of pERK signal in *ben^B* pFCs is indicated in B''' (white dashed line).

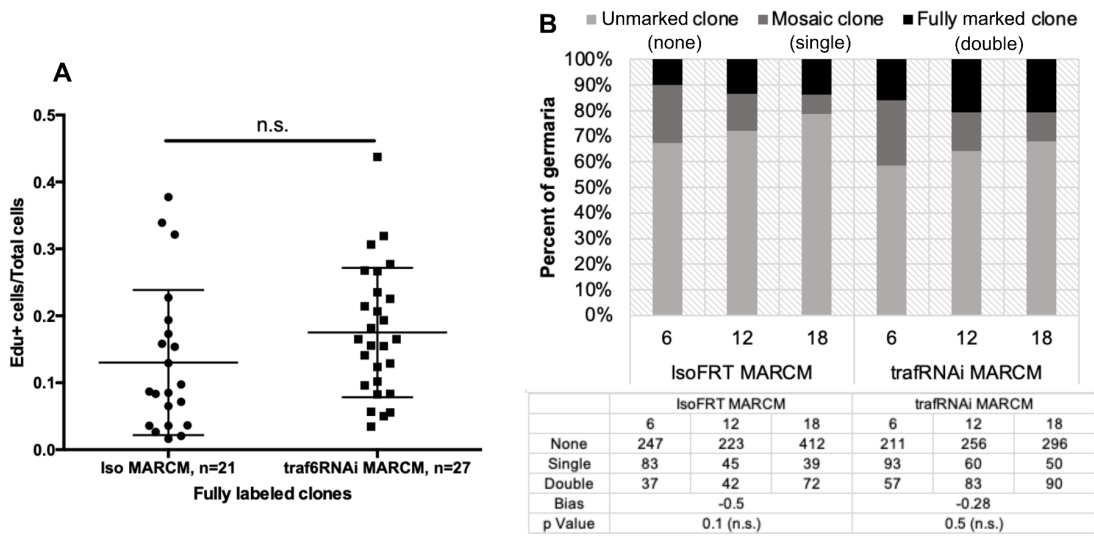


Figure 3.20: Proliferation and competition are not regulated by JNK component and E3 ubiquitin ligase, Traf6, known to interact with Ben.

(A) Proliferation index (Number of Edu+ cells/Total number of cells) calculated for ovarioles with WT clones (Iso MARCM) and *act-gal4>traf6[RNAi]* clones (traf6RNAi MARCM). (B) Quantification of ovarioles with a mosaic or fully-marked clone pattern at 6, 12, and 18 days post heat shock (dphs) of the indicated genotypes. Competition bias (bias) for the indicated genotypes, significance values (p Value), and raw data for competition assays included.

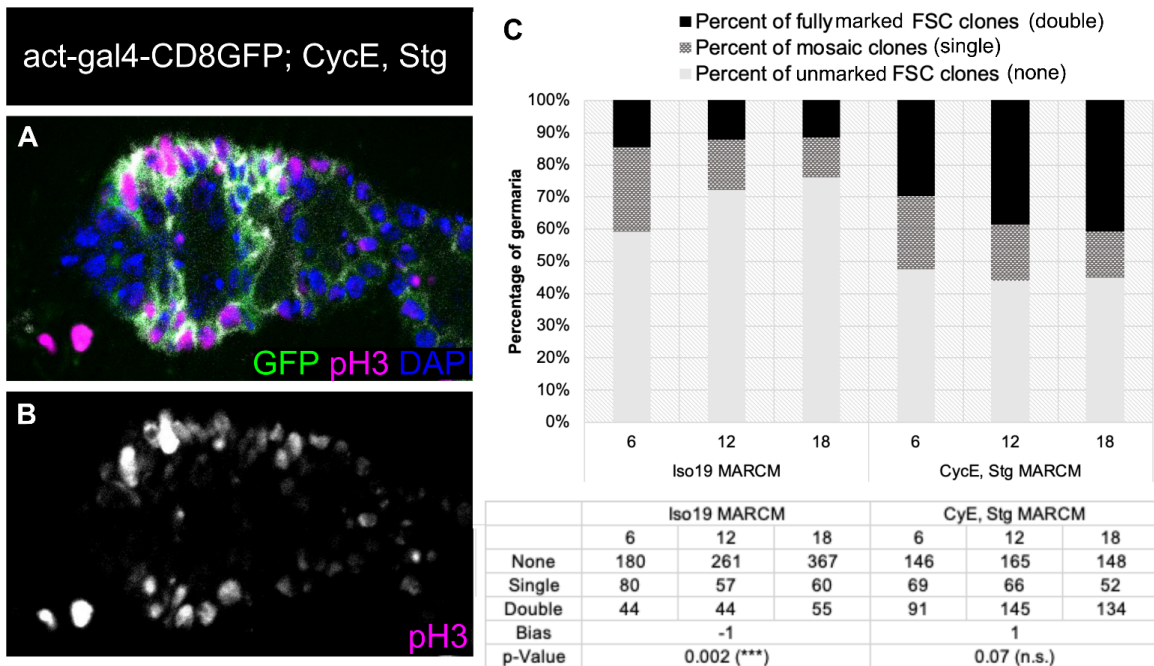


Figure 3.21: Increased proliferation can cause increased FSC competition in the niche.

(A-B) Ovarioles with act-gal4>CycE; Stg clones stained for clonal marker GFP (green), pH3 (marks cells in mitosis, magenta), Fas3 (white), and DAPI (blue). The presence of pERK signal in *ben^B* pFCs is indicated in B''' (white dashed line). (C) Quantification of ovarioles with a mosaic or fully-marked clone pattern at 6, 12, and 18 days post heat shock (dphs) of the indicated genotypes. Competition bias (Bias) for the indicated genotypes, significance values (p Value), and raw data for competition assays included.

Discussion

The segregation of FSC and daughter cell fates requires the orchestration of multiple developmental signaling pathways to ensure that cell fate specification and proliferation occurs at the correct time and place. Here, we have identified a new layer of regulation in which a single gene, *ben*, has multiple distinct roles in promoting differentiation and proliferation in the early FSC lineage.

First, our findings demonstrate that *ben* functions along with the rest of the JNK signaling pathway to promote pFC differentiation. The phenotypes we observed in JNK pathway mutants strongly suggest that the primary defect is a failure to differentiate into mature stalk cells. The range of tube-like and expanded stalk morphological phenotypes we observed could both be explained by an inability of cells in the stalk regions between follicles to facilitate the pinching off of follicles from the germarium or to intercalate into a single row after the pinching off process has been initiated. We cannot rule out the possibility that differentiation toward the polar cell fate or main body cell fate are also impaired upon loss of JNK signaling, but we saw no evidence for this with the markers we used. Notably, although RNAi knockdown of *ben* or *hep* impaired the activity of a reporter for Notch signaling, *NRE-GFP*, in Region 2b pFCs and mature polar cells, this did not seem to interfere with the ability of mutant pFCs to differentiate into polar cells, so the significance of this effect on cell fate specification is unclear. Additional reporters of Notch signaling may help to determine the extent to which Notch signaling is disrupted in these mutant conditions. We also found that pERK is retained in pFCs of ovarioles with impaired JNK signaling, and that constitutive activation of pERK phenocopies the differentiation defects we observed in JNK pathway mutants. These observations suggest that JNK signaling promotes pFC differentiation into stalk cells by inhibiting the activation of ERK in pFCs.

Second, *ben* functions in a JNK-independent manner to help shape the gradient of Hh signaling in FSCs and pFCs. Indeed, we found that levels of *Ptc-pelican-GFP*, indicative of Hh signaling, are higher in *ben* mutant FSCs compared to wild-type, and the *Ptc-pelican-GFP* reporter remains detectable throughout Regions 2b and 3 of the germarium. Likewise, we found that RNAi knockdown of *ben* caused the main body follicle cells to retain *zfh-1* expression, a downstream target of Hh signaling, throughout the germarium and even into Stage 2 in some cases, where it is completely absent in wild-type tissue. However, we also found that *ben* mutant main body follicle cells were able to mature into a Cas⁺, Eya⁻ state, indicating proper differentiation with respect to these two markers. Thus, while loss of *ben* does not fully impair main body follicle cell differentiation, it may influence the process through its role as an upstream regulator of *zfh-1* expression. Further study will be required to understand the functional significance of decreased *cas* and *zfh-1* expression during main body follicle cell differentiation.

JNK signaling has been found to be involved in a wide variety of biological processes in a cell type and context-dependent manner. Some of the most well-known functions of JNK signaling involve responses to non-homeostatic conditions, such as stress, cellular damage, infection, and tumor growth (La Marca and Richardson, 2020; Pinal et al., 2019; Tafesh-Edwards and Eleftherianos, 2020). However, JNK signaling has also been found to be important for processes that occur during normal development or adult homeostasis (Hayes and Solon, 2017; Semba et al., 2020). Indeed, *hep* mutants were originally described for their role in dorsal closure of the epidermis in the embryo (Glise et al., 1995), and subsequent studies have clearly established the importance of the JNK signaling pathway in this process (Hayes and Solon, 2017; Hou et al., 1997; Kockel et al., 1997; Kushnir et al., 2017; Riesgo-Escovar and Hafen, 1997). Likewise, JNK signaling is also important during adult homeostasis in mammalian stem cell lineages, for example to promote self-renewal of human hematopoietic stem cells (Xiao et al., 2019) and differentiation in the mouse intestinal stem cell and human neural stem cell lineages (Bengoa-Vergniory et al., 2014; Sancho et al., 2009). In line with this type of role for JNK signaling, our findings reveal new pathway interactions for JNK signaling in the regulation of cell fate decisions in an epithelial stem cell lineage.

In addition to regulating cell fate decisions, we also identified a JNK-independent role for Ben in the regulation of proliferation rate and FSC niche competition. Previous studies established that increased proliferation causes hypercompetition (Wang et al., 2012), and that the proliferative response to Hh signaling is the key mediator of the FSC niche competition phenotypes in Hh pathway mutants (Huang and Kalderon, 2014). Therefore, the hypercompetition phenotype of *ben* mutant clones is likely caused in large part by the increased Hh signaling levels and proliferation rates in these mutants. Our findings that overexpression of *dap* or RNAi knockdown of *smo* was sufficient to suppress the hypercompetition phenotype of *ben^A* mutant clones are consistent with this. It is possible that delayed differentiation in newly-produced *ben* mutant pFCs also contributes to the hypercompetition phenotype. However, our observation that *hep^{G0107}* mutant clones are not hypercompetitive indicates that the hypercompetition phenotype of *ben* mutant clones is not caused by a block in the JNK-dependent functions of Ben in pFC differentiation.

Taken together, our findings indicate that Ben has JNK-dependent and independent roles in regulating pFC cell fate decisions as they differentiate into polar, stalk and main body follicle cells. Specifically, our findings support a model (Fig. 3.22) in which JNK signaling promotes the differentiation of pFCs during normal homeostasis by helping to downregulate EGFR signaling in early pFCs. Previous studies found that pERK inhibits Groucho and that Groucho is required for the upregulation of Notch signaling in pFCs (Johnston et al., 2016). Thus, the retention of pERK in pFCs may explain why Notch signaling is not upregulated in JNK pathway mutants. Separately, Ben inhibits Hh signaling in a JNK-independent manner, thereby controlling pFC proliferation, regulating FSC niche competition, and possibly contributing to main body follicle cell differentiation. Thus, we have revealed a new layer of regulation within the signaling network that controls cell behavior in the early FSC lineage. The recently published single cell atlases of the adult *Drosophila* ovary (Jevitt et al., 2020; Li et al., 2021; Rust et al., 2020; Slaidina et al., 2021), revealed a continuum of changes in gene expression that occur during cellular differentiation in the early FSC lineage, and provide the tools for characterizing this signaling network in a cell-type

specific manner. In future studies, it will be interesting to apply these new single cell approaches to mutants such as those described here to further elucidate the molecular basis of cell fate decisions in the FSC lineage.

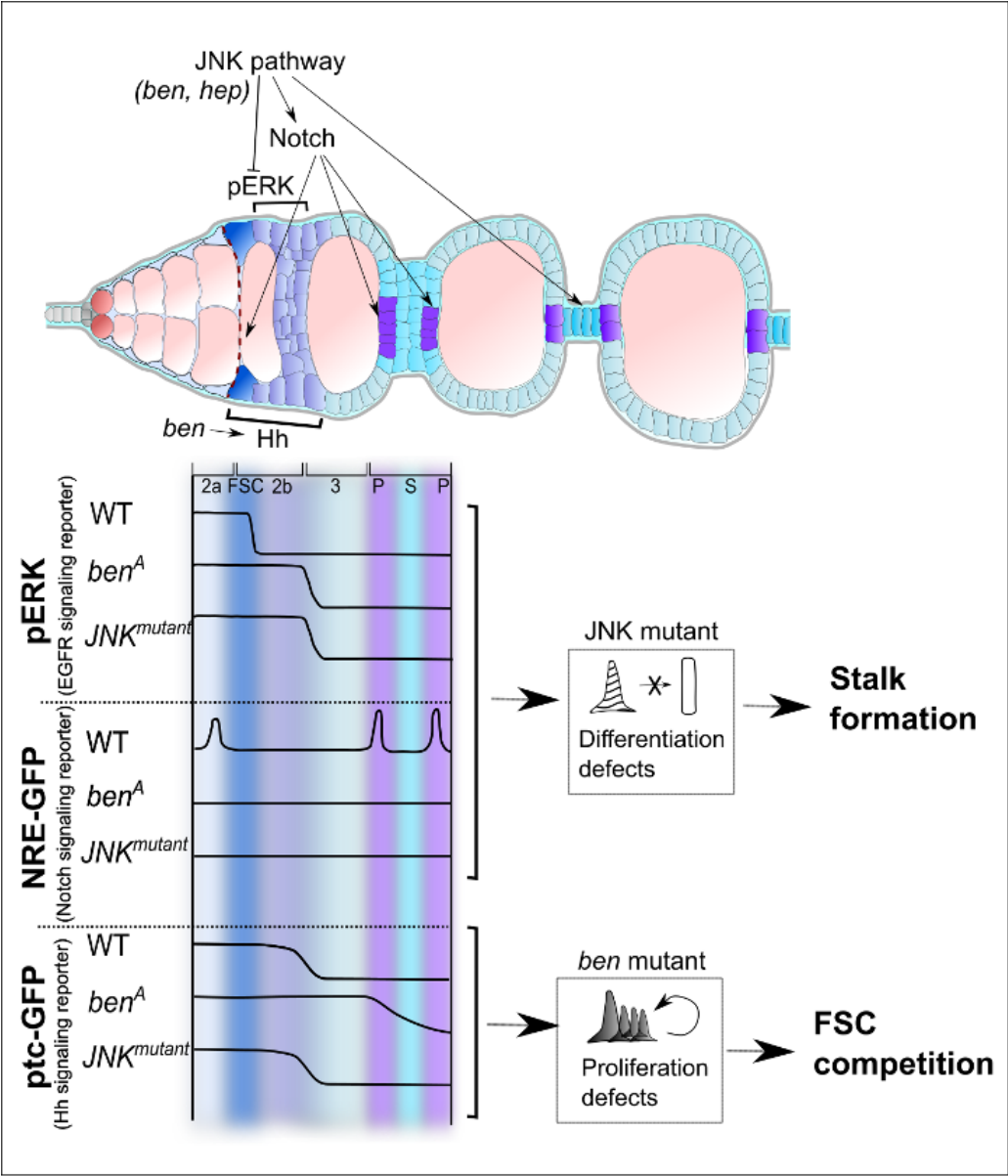


Figure 3.22. Summary of the functions of Ben and JNK pathway genes in the FSC lineage.

Ben positively regulates JNK signaling in the FSC lineage. JNK signaling downregulates the EGFR signaling reporter pERK and may promote Notch signaling in pFCs. In a JNK-independent manner, *ben* downregulates Hh signaling in pFCs. Schematics depict signaling pathway activity profiles in region 2a (2a), FSCs, region 2b (2b), region 3 (3), polar (P) and stalk (S) cells in the FSC lineage. In schematics for

each genotype, an increase or decrease in reporter signal (black line) is represented. pERK is detectable in IGS cells in Region 2a and FSCs at the 2a/b border, but is undetectable in early pFCs. *NRE-GFP*, a reporter for Notch signaling, is first detected along the 2a/b border, and then detected in mature polar cell clusters. *Ptc-GFP*, a reporter for Hh signaling activity, gradually decreases from IGS cells in Region 2a to early pFCs in Region 2b. Loss of JNK signaling leads to delays in differentiation and results in pFC differentiation defects. Loss of *ben* also leads to perdurance of Hh signaling beyond region 2b contributing to defects in differentiation and proliferation. Increased proliferation in *ben* mutants leads to FSC hypercompetition.

Future directions:

Several questions with regards to the precise mechanism by which the E2 ubiquitin ligase functionality of *ben* mediates effects on differentiation and competition, warrant further investigation. Open questions include:

- (a) Which E3 ubiquitin ligases does Ben interact with to affect EGFR, Notch and Hh signaling pathways?
- (b) What is the functional significance of the expanded pERK phenotype in pFCs? How does it influence pFC cell fate specification? Could pFCs that retain pERK be an intermediate cell fate between FSCs and early pFCs?
- (c) How do the different signaling pathways necessary for regulating FSC differentiation interact and affect each other?
- (d) What are the rules underlying FSC niche competition?
- (e) What are the mechanics of FCs resulting in differentiation phenotypes including expanded stalk and tube-like phenotypes? How are these seemingly contrasting phenotypes caused as a result of loss of Bendless?

In future studies, it will be interesting to investigate these questions. Recent single-cell sequencing efforts championed by the lab have provided an insight into transcriptional profiles for different cell types in the FSC lineage. These efforts along with the current focus of the Nystul lab on developing robust live-imaging techniques to visualize FSC differentiation and FSC niche dynamics will lead to the development of tools that make it possible to thoroughly investigate these questions in subsequent studies.

Chapter 4

Retinoblastoma factor, Rbf

Among the strongest hits from the screen was an allele of *retinoblastoma-family protein (rbf)*. The allele, *rbf^A*, contains a single nonsense mutation in the C-terminal domain of the protein and is homozygous lethal. In the screen conducted by Cook et al., 2018, *rbf^A* mutant FSCs scored as a candidate for FSC hypercompetition. Rbf negatively regulates E2F, a cell cycle regulator that regulates G1 exit in the cycle (Mouawad, R., et al., 2020). Rbf mutants have been characterized for their role affecting S-phase progression in *Drosophila* embryonic and eye development (Payankaulam, S. et al., 2016). During *Drosophila* wing development, Rbf1-induced JNK-dependent apoptosis has been found to activate compensatory proliferation (Clavier, A., et al., 2016). In addition, Rbf is necessary for cyst and germline stem cell differentiation in the *Drosophila* testis (Dominado, N., et al., 2016, Greenspan, L. J. and Matunis, E. L., 2018).

Rbf is necessary for FSC differentiation

In order to further investigate the role of Rbf in FSC differentiation and competition, we stained ovarioles with *rbf[RNAi]* driven in early follicle cells specifically during adulthood using *10930-Gal4* and *tub-Gal80^{ts}* for Fas3, which marks membranes of early follicle cells, and examined the tissue morphology. We found that germaria displayed a range of phenotypes including side-by-side egg chamber phenotype, referred to as “double germarium”, fused egg-chambers, epithelial gaps in main body epithelium and an expanded stalk-like phenotype. Additionally, we stained ovarioles with early differentiation markers Castor (Cas) and Eyes-absent (Eya). We found that Eya is misexpressed in stalk cells, leading to Cas⁺ Eya⁺ stalk cells in germaria that did not display any evident morphological phenotypes, and in those that displayed phenotypes. Together, these results indicate that Rbf is necessary for normal FSC differentiation (Fig. 4.1).

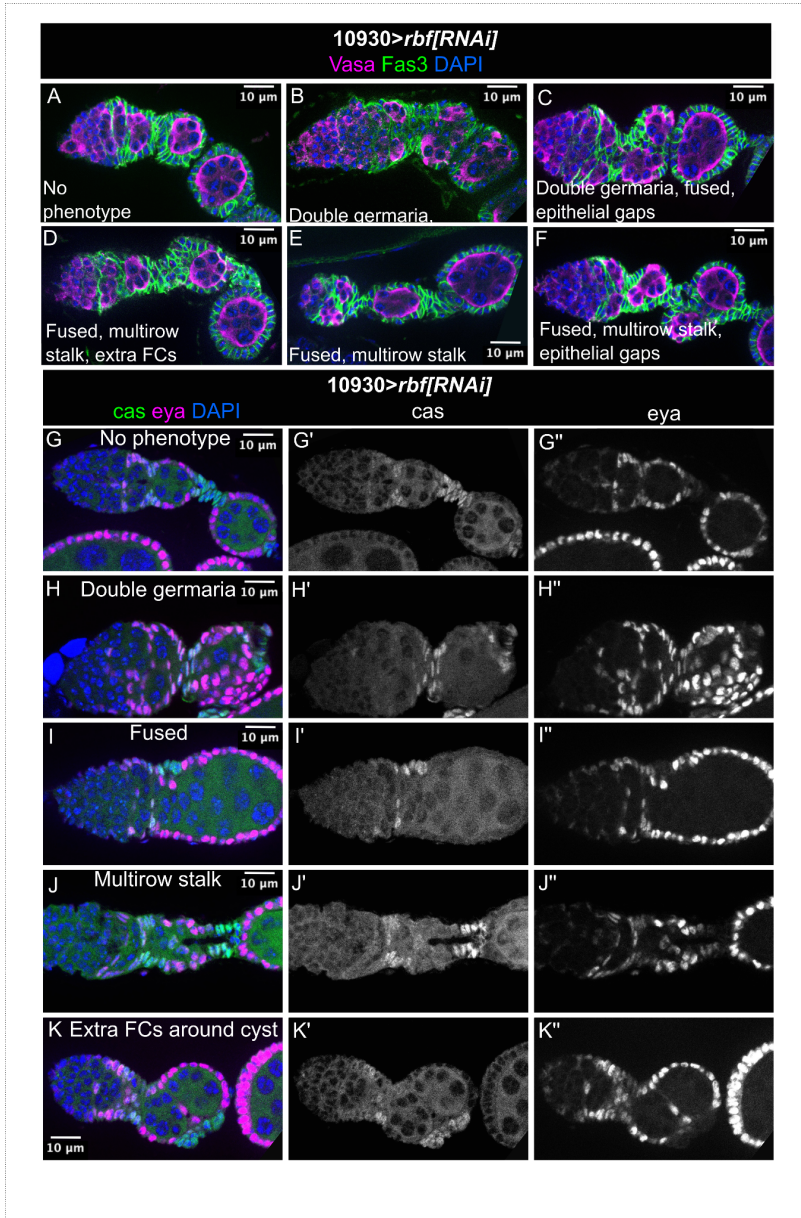


Figure 4.1. Loss of Rbf results in differentiation defects

(A-F) Ovarioles with *109-30^{ts}* expressing *rbf[RNAi]* stained with Vasa (magenta), Fas3 (green) and DAPI (nuclei). (G-K) Ovarioles with *109-30^{ts}* expressing *rbf[RNAi]* stained with Eya (magenta), Cas (green) and DAPI (nuclei).

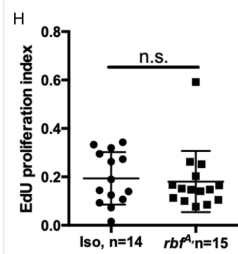
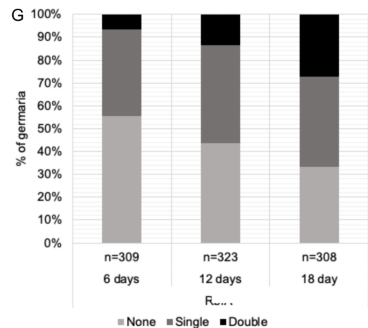
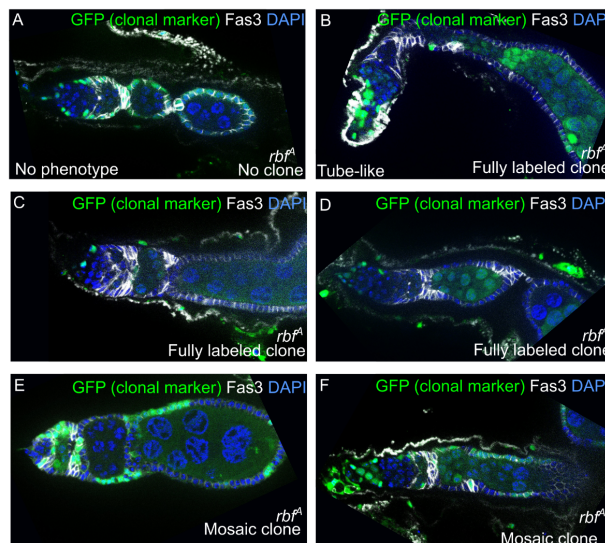
Loss of Rbf causes FSC hypercompetition

To confirm the hypercompetition phenotype of *rbf^A*, we heat shocked flies to induce wildtype control or *rbf^A* mutant clones that are marked by the lack of GFP in adult flies, and quantified the proportion of germaria with fully GFP⁻, mosaic, or fully GFP⁺ follicle cell populations at 6, 12 and 18 days post heat

shock (dphs). We observed a significant increase in germaria with *rbf^A* mutant clones compared to wildtype, indicating that *rbf^A* mutant cells are hypercompetitive for the FSC niche and displayed morphological phenotypes in germaria (Fig. 4.2).

Loss of Rbf does not affect FC proliferation

Given previous evidence for the role of Rbf in regulating cell cycle progression, we used EdU assays, which identify cells in S-phase in ovarioles with wildtype and *rbf^A* clones. Surprisingly, we observed no significant difference in the percentages of EdU+ cells (i.e. the proliferation indices) between both genotypes (Fig. 4.2H).



rbf^A lifespan assay
bias = 100%, p = 6.30e-07

	6 dphs n=309	12 dphs n=323	18 dphs n=308
Unlabeled (no clones)	172	141	103
Mosaic clones	117	138	121
Fully labeled clones	20	44	84

Figure 4.2. *rbf^A* mutant FSCs are hypercompetitive and not overproliferative

(A-F) Ovarioles containing *rbf^A* mutant clones stained with GFP clonal marker (green), Fas3 (white), DAPI (blue). (G) Quantification of ovarioles with a mosaic or fully-marked clone pattern at 6, 12, and 18 days post heat shock (dphs) of the indicated genotypes. Competition bias (bias) for the indicated genotypes, significance values (p), and raw data for competition assays included. (H) Proliferation index (Number of Edu+ cells/Total number of cells) calculated for ovarioles with WT clones (Iso MARCM) and *rbf^A* mutant clones.

Future directions:

While these data only mark the start of an investigation into the role of Rbf in regulating FSC competition and differentiation, a further investigation into the underlying mechanism for hypercompetition in *rbf* mutants is warranted. Moreover, performing single cell analyses on *ben* and *rbf* mutants, along with other confirmed hyper- and hypo- competitors will enable an examination of commonalities and differences between regulator mechanisms for FSC hypercompetition and hypo-competition. These efforts might be significantly valuable to uncover an in-depth understanding of the processes underlie the dynamics in the FSC niche. Developing live imaging techniques to visualize mutants that are candidate hypercompetitors and hypo-competitors might also be helpful in providing exciting advances in our understanding of mechanisms for competition.

Chapter 5

Materials and Methods

Fly husbandry and stocks

All fly stocks were maintained on standard molasses food at 25°C. For experiments with flies that have *tub-Gal80^{ts}*, the crosses were performed at 18°C and adults were shifted to 29°C for 14 days, unless specified otherwise. For experiments with clones, flies were dissected at 12 days post clone induction, unless specified otherwise. Bloomington Drosophila Stock Center (BDSC), Vienna Drosophila Resource Center (VDRC), Kyoto Stock Center (Kyoto).

IsoFRT19A (BDSC #1744); *ben^A*, *FRT19A* (BDSC #57057); *hsFlp*, *Ubi-GFP*, *FRT19A*; *109-30-Gal4*, *tub-gal80^{ts}* (generated from BDSC #7019 and #7023); *UAS-ben[RNAi]* (VDRC #109638); *AP-1-GFP* kindly provided by the Hariharan Lab, University of California, Berkeley (Chatterjee and Bohmann, 2012; Harris et al., 2016); *hsFlp*, *Ubi-RFP*, *FRT19A* (BDSC #31418); *UAS-hep[RNAi]* (VDRC #109277); *NRE-pGR*, referred to as NRE-GFP; *hep^{G0107}*, *FRT19A* (Kyoto #111740); *UAS-egr[RNAi]* (VDRC #108814); *UAS-grnd[RNAi]* (VDRC #104538); *UAS-traf6[RNAi]* (VDRC #110266); *Canton-S*; *UAS-ERK^{SEM}* (VDRC #59006); *w^t**; *Ptc-pelican-GFP* generated in and kindly provided by the Kornberg lab, University of California, San Francisco (Sahai-Hernandez and Nystul, 2013); *w^t**; *UAS-Hh::eGFP/CyO* (BDSC #81024); *UAS-dap* kindly provided by the Buttitta lab, University of Michigan (Lane et al., 1996); *hsFlp*, *tub-Gal80*, *FRT19A*; *Act5C-Gal4*, *UAS-CD8-GFP* (generated from BDSC #42726 and #44407); *UAS-smo[RNAi]* (BDSC #27037); *ben^B* (BDSC #57058); *UAS-bsk[RNAi]* (VDRC #104569); *10X-STAT-GFP* (BDSC #26197); *stl-Gal4* (BDSC #77732).

Immunostaining and imaging

Flies were dissected in 1X PBS at room temperature, samples were fixed for 15 minutes in 1X PBS with 4% paraformaldehyde and then rinsed twice with 1X PBS. Samples were blocked for 1 hour at room

temperature in block solution (1X PBS containing 0.2% Triton X-100 (PBST) and 0.5% bovine serum albumin). Samples were incubated overnight at 4°C with primary antibody diluted in block solution. Next, samples were rinsed twice and then incubated for 1 hour at room temperature with block solution. Samples were incubated overnight at 4°C with secondary antibody diluted in block solution. Next, samples were rinsed twice with 1X PBST and then rinsed once with 1X PBS. Samples were mounted in DAPI Fluoromount-G (Thermo Fisher Scientific, OB010020).

The following primary antibodies were used: mouse anti-Fas3 (1:50; DSHB, 7G10), guinea pig anti-GFP (1:1000; Synaptic Systems, 132005), guinea pig anti-Zfh-1 (1:500; a gift from James Skeath), rabbit anti-GFP (1:1000; Torrey Pines Biolabs Inc., TP-401), mouse anti-Eya (1:50; DSHB, 10H6), rabbit anti-Castor (1:5000; a gift from Ward Odenwald and Jonathan Benito Sipos), rat anti-RFP (1:1000; ChromoTek, 5F8), rabbit anti-pERK (1:100; Cell Signaling Technology, 4370), guinea pig anti-Traffic Jam (1:5000, gift from Dorothea Godt), rabbit anti-Bazooka (Baz, 1:1000, a gift from Andreas Wodarz), rat anti-DE-Cadherin (Shotgun, 1:100, DSHB, DCAD2), mouse anti-Discs Large (Dlg, 1:200, DSHB, 4F3). The following secondary antibodies were purchased from Thermo Fisher Scientific and used at 1:1000: goat anti-guinea pig 488 (A-11073), goat anti-guinea pig 633 (A-21450), goat anti-rabbit 488 (A-11008), goat anti-rabbit 555 (A-21428), goat anti-mouse 488 (A-11029), goat anti-mouse 555 (A-21424), goat anti-mouse 647 (A-21236), goat anti-mouse 555 (A-21236) and goat anti-rat 555 (A-21434).

Samples were imaged using a Zeiss M2 Axioimager with Apotome unit, Nikon C1si Spectral Confocal microscope or SP5 line-scanning confocal microscope. Image processing was done using FIJI and Inkscape.

EdU staining

For EdU assays, ovaries were dissected in 1X PBS and incubated in 1X PBS containing 15 μ M EdU (Click-it EdU Alexa Fluor 555 Imaging Kit, Life Technologies, C10338) at room temperature for 1 hour. Samples were rinsed twice with 1X PBS and fixed in 4% paraformaldehyde for 15 minutes. To permeabilize

samples, ovaries were washed twice in 1X block (0.5% BSA in PBST) and incubated in fresh block solution for 1 hour at room temperature. Then, samples were incubated overnight at 4°C with primary antibody solution. Next, samples were washed twice in 1X block for 10 minutes then incubated in a Click-iT reaction cocktail (1× Click-iT EdU reaction buffer, CuSO₄, 555-Alexa Fluor azide, 1× Click-iT EdU buffer additive) for 30 minutes at room temperature, protected from light. Samples were rinsed twice with 1X block then washed for 1 hour in fresh block solution at room temperature. Samples were incubated overnight at 4°C in secondary antibody solution. Finally, samples were rinsed with 1X PBS and mounted using DAPI Fluoromount-G.

EdU proliferation index analysis

Images of ovarioles stained with Traffic Jam (Tj), a marker for somatic cell nuclei, and EdU, a marker for cells in S-phase, were analyzed using Imaris, as described previously (Fadiga and Nystul, 2019). Briefly, the Tj channel was processed for background subtraction, the surfaces tool was used to segment the images, and surfaces were used to quantify cell number and signal intensities. In mosaic clones, we determined the number of GFP⁺ and GFP⁻ cells, by (1) measuring the intensity of GFP within each surface; (2) determining the threshold of GFP intensity that distinguishes GFP⁺ cells from GFP⁻ cells, as determined by visual inspection of the image sets; and (3) quantifying the number of surfaces above and below the threshold. The mean intensity of the EdU signal in each surface was then used to identify EdU⁺ cells. The EdU proliferation index was calculated by determining the ratio of the total number of EdU⁺ cells to the total number of cells in 2b. In mosaics, the total number of surfaces in 2b, pertains to the total number of GFP⁺ or GFP⁻ cells in Region 2b.

Hybridization Chain Reaction

Probes sets of 20 probes per gene were custom made by Molecular Instruments. For *ben*, a sequence (X:13991931..14005990 from release 6.37) that is shared by all isoforms was submitted. For *hep*, the sequence of the hep-RA isoform (accession # NM_167346) was used. Prior to dissections, experimental

flies were fed with molasses food and wet yeast for at least 3 consecutive days. The hybridization chain reaction (HCR) protocol (Choi et al., 2018) was adapted for use in *Drosophila* ovaries, as described previously (Slaidina et al., 2020; Slaidina et al., 2021). On the first day, fly ovaries were dissected in DPBS (CaCl₂, MgCl₂ free) on ice. Samples were fixed in solution containing DPBS, 0.1% Tween, and 4% paraformaldehyde for 20 minutes at room temperature. All subsequent steps were carried out in RNA-ase free conditions, using reagents specified and supplied from the Molecular Instruments HCR v3.0 kit. Samples were permeabilized by rinsing twice with wash solution containing DPBS and 0.1% Tween at room temperature. Samples were then dehydrated on ice with sequential 20-minute washes with solutions containing 25%, 50%, 75% and 100% methanol diluted in DPBS (in the order specified). The wash with 100% methanol was carried out twice. The samples were then stored overnight at -20°C. On the second day, samples were re-hydrated on ice with 20 -minute sequential washes with solutions containing 100%, 75%, 50%, 25% and 0% methanol in DPBS (in the order specified). Samples were washed for 2 hours with a DPBS solution with 1% Triton-X. Then, samples were fixed in a solution containing DPBS, 0.1% Tween and 4% paraformaldehyde for 20 minutes at room temperature. Samples were washed for 5 minutes with wash solution (DPBS containing 0.1% Tween) two times on ice. Then, the samples were transferred to RNA-ase free eppendorf tubes and incubated in a probe hybridization solution (containing a pre-warmed probe hybridization buffer mixed with 4-8pmols of probe sets) for 24 hours at 37°C. On the third day, samples underwent four 15-minute washes with probe wash buffer solution. Samples were washed for 5 minutes with 5X SSCT at room temperature, followed by a 5-minute incubation in pre-amplification buffer. Then, samples were incubated in light protected conditions for 16 hours at room temperature in a hairpin solution (prepared by diluting snap-cooled hairpins in the pre-amplification buffer). On the next day, samples were washed twice for 5 minutes, twice for 30 minutes and lastly for 5 minutes with 5X SSCT. Then, DAPI Fluoromount-G was added and samples were mounted for imaging and analysis.

Clone induction

Newly eclosed adults of appropriate genotypes were collected and transferred to empty vials and capped with cotton balls (instead of vial plugs). Flies were heat shocked by submerging vials into a 37°C water bath for 50 minutes to 1 hour. Vials were removed and flies were transferred into vials with wet yeast and allowed to recover at room temperature for at least 6 hours. This process was repeated twice, on two consecutive days. Flies were then incubated at 25°C and fed wet yeast daily. Flies were fed daily for at least 2 days preceding all experiments involving dissections.

FSC competition assay

Negatively marked clones and positively marked MARCM clones were generated using the clone induction protocol described above. The clone induction protocol results in germaria with fully marked, mosaic or unmarked stem cell clones. The frequency of clones in each of these categories were measured at 6, 12, and 18 days post clone induction (counted from the second day of heat shock). Over time, mosaic germaria can either become unmarked germaria or fully marked clones, indicating that stem cell replacement has occurred. An increase in the proportion of fully marked germaria is related to the rate of clone expansion, whereas an increase in the proportion of unmarked germaria is related to the rate of clone extinction. In wild-type tissue, the rates of extinction and expansion are approximately equal. Homozygosity for a mutation that promotes FSC retention in the niche or self-renewal will cause the rate of clonal expansion to be higher than the rate of clone extinction, resulting in FSC hypercompetition. Competition bias, b , was calculated as described previously (Kronen et al., 2014).

Statistics and graphs

Student's t-tests and Pearson's Chi-squared tests were used to calculate 95% confidence intervals and determine p-values using GraphPad Prism 6. Competition bias values, b , along with associated p-values were calculated as previously described in Kronen et al. 2014. Bias was calculated using a MatLab script (Kronen et al., 2014). Comparisons between genotypes at individual time points was done using a Pearson's

Chi-squared test in R. In all stacked graphs, cumulative percentages of indicated phenotypes have been represented. In bar graphs, individual dots represent percentages of phenotypes in each fly examined, and the bar height represents the mean percent of indicated phenotypes across replicates. The error bars shown in graphs represent standard deviation. Standard deviation was not calculated when Chi-squared tests were done. Multiple flies (N) were examined for each experiment and the ovariole number (n) equals the total number of ovarioles observed from all flies. No data points were excluded. Samples were not randomized or blinded. Raw data for all the quantifications have been provided in the supplemental materials.

References

- Assa-Kunik, E., Torres, I., Schejter, E., Johnston, D. and Shilo, B.** (2007). Drosophila follicle cells are patterned by multiple levels of Notch signaling and antagonism between the Notch and JAK/STAT pathways. *Development* **134**, 1161–1169.
- Bach, E. A., Ekas, L. A., Ayala-Camargo, A., Flaherty, M. S., Lee, H., Perrimon, N. and Baeg, G.-H.** (2007). GFP reporters detect the activation of the Drosophila JAK/STAT pathway in vivo. *Gene Expr. Patterns* **7**, 323–331.
- Bai, J. and Montell, D.** (2002). Eyes absent, a key repressor of polar cell fate during Drosophila oogenesis. *Development* **129**, 5377–5388.
- Baril, C., Sahmi, M., Ashton-Beaucage, D., Stronach, B. and Therrien, M.** (2009). The PP2C Alphabet is a negative regulator of stress-activated protein kinase signaling in Drosophila. *Genetics* **181**, 567–579.
- Bengoa-Vergniory, N., Gorroño-Etxebarria, I., González-Salazar, I. and Kypta, R. M.** (2014). A switch from canonical to noncanonical Wnt signaling mediates early differentiation of human neural stem cells. *Stem Cells* **32**, 3196–3208.
- Berns, N., Woichansky, I., Friedrichsen, S., Kraft, N. and Riechmann, V.** (2014). A genome-scale in vivo RNAi analysis of epithelial development in Drosophila identifies new proliferation domains outside of the stem cell niche. *J. Cell Sci.* **127**, 2736–2748.
- Carpenter, A. T. C.** (1975). Electron microscopy of meiosis in *Drosophila melanogaster* females. *Chromosoma* **51**, 157–182.
- Casey, J. R., Grinstein, S., & Orlowski, J.** (2009). Sensors and regulators of intracellular pH. *Nature Reviews Molecular Cell Biology* *Nat Rev Mol Cell Biol*, 11(1), 50-61. doi:10.1038/nrm2820

- Castanieto, A., Johnston, M. J. and Nystul, T. G.** (2014). EGFR signaling promotes self-renewal through the establishment of cell polarity in *Drosophila* follicle stem cells. *Elife* **3**,.
- Chang, Y.-C., Jang, A. C.-C., Lin, C.-H. and Montell, D. J.** (2013). Castor is required for Hedgehog-dependent cell-fate specification and follicle stem cell maintenance in *Drosophila* oogenesis. *Proc. Natl. Acad. Sci. U. S. A.* **110**, E1734–42.
- Chatterjee, N. and Bohmann, D.** (2012). A versatile Φ C31 based reporter system for measuring AP-1 and Nrf2 signaling in *Drosophila* and in tissue culture. *PLoS One* **7**, e34063.
- Chen, Y.** (2000) Soluble Adenylyl Cyclase as an Evolutionarily Conserved Bicarbonate Sensor. *Science* **289**, 625–628.
- Choi, H. M. T., Schwarzkopf, M., Fornace, M. E., Acharya, A., Artavanis, G., Stegmaier, J., Cunha, A. and Pierce, N. A.** (2018). Third-generation in situ hybridization chain reaction: multiplexed, quantitative, sensitive, versatile, robust. *Development* **145**,.
- Clayton, E., Doupé, D. P., Klein, A. M., Winton, D. J., Simons, B. D. and Jones, P. H.** (2007). A single type of progenitor cell maintains normal epidermis. *Nature* **446**, 185–189.
- Cook, M. S., Cazin, C., Amoyel, M., Yamamoto, S., Bach, E. and Nystul, T.** (2017). Neutral Competition for *Drosophila* Follicle and Cyst Stem Cell Niches Requires Vesicle Trafficking Genes. *Genetics* **206**, 1417–1428.
- Dai, W., Peterson, A., Kenney, T., Burrous, H. and Montell, D. J.** (2017). Quantitative microscopy of the *Drosophila* ovary shows multiple niche signals specify progenitor cell fate. *Nat. Commun.* **8**, 1244.
- Denker, S. P. & Barber, D. L.** Cell migration requires both ion translocation and cytoskeletal anchoring by the Na-H exchanger NHE1. *The Journal of cell biology* **159**, 1087–96 (2002).

- Erecińska, M., Deas, J. & Silver, I.** (1995) The effect of pH on glycolysis and phosphofructokinase activity in cultured cells and synaptosomes. *Journal of neurochemistry* **65**, 2765–72.
- Ek-Vitorín, J. F. et al.** PH regulation of connexin43: molecular analysis of the gating particle. *Biophysical journal* **71**, 1273–84 (1996).
- Fadiga, J. and Nystul, T. G.** (2019). The follicle epithelium in the *Drosophila* ovary is maintained by a small number of stem cells. *Elife* **8**,.
- Fox, D. T., Morris, L. X., Nystul, T. and Spradling, A. C.** (2008). *StemBook*. Cambridge (MA): Harvard Stem Cell Institute.
- Frantz, C. et al.** Cofilin is a pH sensor for actin free barbed end formation: role of phosphoinositide binding. *The Journal of cell biology* **183**, 865–79 (2008).
- Glise, B., Bourbon, H., and Noselli, S.** (1995). hemipterous encodes a novel *Drosophila* MAP kinase kinase, required for epithelial cell sheet movement. *Cell* **83**, 451–461.
- González-Nieto, D. et al.** Regulation of neuronal connexin-36 channels by pH. *Proceedings of the National Academy of Sciences of the United States of America* **105**, 17169–74 (2008).
- Guichard, A., Park, J. M., Cruz-Moreno, B., Karin, M. and Bier, E.** (2006). *Anthrax lethal factor and edema factor act on conserved targets in Drosophila*. *Proc. Natl. Acad. Sci. U. S. A.* **103**, 3244–3249.
- Hafezi, Y. and Nystul, T. G.** (2001). Advanced Techniques for Cell Lineage Labelling in *Drosophila*. *Multiple values selected*.
- Harris, R. E., Setiawan, L., Saul, J. and Hariharan, I. K.** (2016). Localized epigenetic silencing of a damage-activated WNT enhancer limits regeneration in mature *Drosophila* imaginal discs. *Elife* **5**,.

- Hartman, T. R., Zinshteyn, D., Schofield, H. K., Nicolas, E., Okada, A. and O'Reilly, A. M.** (2010). *Drosophila* Boi limits Hedgehog levels to suppress follicle stem cell proliferation. *J. Cell Biol.* **191**, 943–952.
- Hartman, T. R., Strohlic, T. I., Ji, Y., Zinshteyn, D. and O'Reilly, A. M.** (2013). Diet controls *Drosophila* follicle stem cell proliferation via Hedgehog sequestration and release. *J. Cell Biol.* **201**, 741–757.
- Hayes, P. and Solon, J.** (2017). *Drosophila* dorsal closure: An orchestra of forces to zip shut the embryo. *Mech. Dev.* **144**, 2–10.
- Herrera, S. C. and Bach, E. A.** (2021). The Emerging Roles of JNK Signaling in *Drosophila* Stem Cell Homeostasis. *Int. J. Mol. Sci.* **22**,.
- Hou, X. S., Goldstein, E. S. and Perrimon, N.** (1997). *Drosophila* Jun relays the Jun amino-terminal kinase signal transduction pathway to the Decapentaplegic signal transduction pathway in regulating epithelial cell sheet movement. *Genes Dev.* **11**, 1728–1737.
- Housden, B. E., Millen, K. and Bray, S. J.** (2012). *Drosophila* Reporter Vectors Compatible with ΦC31 Integrase Transgenesis Techniques and Their Use to Generate New Notch Reporter Fly Lines. *G3* **2**, 79–82.
- Huang, J. and Kalderon, D.** (2014). Coupling of Hedgehog and Hippo pathways promotes stem cell maintenance by stimulating proliferation. *J. Cell Biol.* **205**, 325–338.
- Jevitt, A., Chatterjee, D., Xie, G., Wang, X.-F., Otwell, T., Huang, Y.-C. and Deng, W.-M.** (2020). A single-cell atlas of adult *Drosophila* ovary identifies transcriptional programs and somatic cell lineage regulating oogenesis. *PLoS Biol.* **18**, e3000538.

- Johnston, M. J., Bar-Cohen, S., Paroush, Z. and Nystul, T. G.** (2016). Phosphorylated Groucho delays differentiation in the follicle stem cell lineage by providing a molecular memory of EGFR signaling in the niche. *Development* **143**, 4631–4642.
- Kim-Yip, R. P. and Nystul, T. G.** (2018). Wingless promotes EGFR signaling in follicle stem cells to maintain self-renewal. *Development* **145**,.
- Klein, A. M. and Simons, B. D.** (2011). Universal patterns of stem cell fate in cycling adult tissues. *Development* **138**, 3103–3111.
- Koch, E. A. and King, R. C.** (1966). The origin and early differentiation of the egg chamber of *Drosophila melanogaster*. *J. Morphol.* **119**, 283–303.
- Kockel, L., Zeitlinger, J., Staszewski, L. M., Mlodzik, M. and Bohmann, D.** (1997). Jun in *Drosophila* development: redundant and nonredundant functions and regulation by two MAPK signal transduction pathways. *Genes Dev.* **11**, 1748–1758.
- Kronen, M. R., Schoenfelder, K. P., Klein, A. M. and Nystul, T. G.** (2014). Basolateral junction proteins regulate competition for the follicle stem cell niche in the *Drosophila* ovary. *PLoS One* **9**, e101085.
- Kushnir, T., Mezuman, S., Bar-Cohen, S., Lange, R., Paroush, Z. 'ev and Helman, A.** (2017). Novel interplay between JNK and Egfr signaling in *Drosophila* dorsal closure. *PLoS Genet.* **13**, e1006860.
- La Marca, J. E. and Richardson, H. E.** (2020). Two-Faced: Roles of JNK Signalling During Tumourigenesis in the *Drosophila* Model. *Front Cell Dev Biol* **8**, 42.

- Lane, M. E., Sauer, K., Wallace, K., Jan, Y. N., Lehner, C. F. and Vaessin, H.** (1996). Dacapo, a cyclin-dependent kinase inhibitor, stops cell proliferation during *Drosophila* development. *Cell* **87**, 1225–1235.
- Lee, T. and Luo, L.** (2001). Mosaic analysis with a repressible cell marker (MARCM) for *Drosophila* neural development. *Trends Neurosci.* **24**, 251–254.
- Li, H., Janssens, J., De Waegeneer, M., Kolluru, S. S., Davie, K., Gardeux, V., Saelens, W., David, F., Brbić, M., Leskovec, J., et al.** (2021). Fly Cell Atlas: a single-cell transcriptomic atlas of the adult fruit fly. *bioRxiv* 2021.07.04.451050.
- Lopez-Schier, H. and St Johnston, D.** (2001). Delta signaling from the germ line controls the proliferation and differentiation of the somatic follicle cells during *Drosophila* oogenesis. *Genes Dev.* **15**, 1393–1405.
- Ma, X., Li, W., Yu, H., Yang, Y., Li, M., Xue, L. and Xu, T.** (2014). Bendless modulates JNK-mediated cell death and migration in *Drosophila*. *Cell Death Differ.* **21**, 407–415.
- Margolis, J. and Spradling, A.** (1995). Identification and behavior of epithelial stem cells in the *Drosophila* ovary. *Development* **121**, 3797–3807.
- McGuire, S. E., Le, P. T., Osborn, A. J., Matsumoto, K. and Davis, R. L.** (2003). Spatiotemporal rescue of memory dysfunction in *Drosophila*. *Science* **302**, 1765–1768.
- Melamed, D. and Kalderon, D.** (2020). Opposing JAK-STAT and Wnt signaling gradients define a stem cell domain by regulating differentiation at two borders. *Elife* **9**,.
- Michel, M., Kupinski, A. P., Raabe, I. and Bökel, C.** (2012). Hh signalling is essential for somatic stem cell maintenance in the *Drosophila* testis niche. *Development* **139**, 2663–2669.

- Miller, A.** (1950). The internal anatomy and histology of the imago of *Drosophila melanogaster*. *The Biology of Drosophila* 421–534.
- Nystul, T. G. and Spradling, A.** (2007). An epithelial niche in the *Drosophila* ovary undergoes long-range stem cell replacement. *Cell Stem Cell* **1**, 277–285.
- Nystul, T. G. and Spradling, A.** (2010). Regulation of epithelial stem cell replacement and follicle formation in the *Drosophila* ovary. *Genetics* **184**, 503–515.
- Pinal, N., Calleja, M. and Morata, G.** (2019). Pro-apoptotic and pro-proliferation functions of the JNK pathway of *Drosophila*: roles in cell competition, tumorigenesis and regeneration. *Open Biol.* **9**, 180256.
- Riesgo-Escovar, J. R. and Hafen, E.** (1997). *Drosophila* Jun kinase regulates expression of decapentaplegic via the ETS-domain protein Aop and the AP-1 transcription factor DJun during dorsal closure. *Genes Dev.* **11**, 1717–1727.
- Rust, K. and Nystul, T.** (2020). Signal transduction in the early *Drosophila* follicle stem cell lineage. *Current Opinion in Insect Science* **37**, 39–48.
- Rust, K., Byrnes, L. E., Yu, K. S., Park, J. S., Sneddon, J. B., Tward, A. D. and Nystul, T. G.** (2020). A single-cell atlas and lineage analysis of the adult *Drosophila* ovary. *Nat. Commun.* **11**, 5628.
- Sahai-Hernandez, P. and Nystul, T. G.** (2013). A dynamic population of stromal cells contributes to the follicle stem cell niche in the *Drosophila* ovary. *Development* **140**, 4490–4498.
- Sancho, R., Nateri, A. S., de Vinuesa, A. G., Aguilera, C., Nye, E., Spencer-Dene, B. and Behrens, A.** (2009). JNK signalling modulates intestinal homeostasis and tumourigenesis in mice. *EMBO J.* **28**, 1843–1854.

- Semba, T., Sammons, R., Wang, X., Xie, X., Dalby, K. N. and Ueno, N. T.** (2020). JNK Signaling in Stem Cell Self-Renewal and Differentiation. *Int. J. Mol. Sci.* **21**,.
- Singh, T., Lee, E. H., Hartman, T. R., Ruiz-Whalen, D. M. and O'Reilly, A. M.** (2018). Opposing Action of Hedgehog and Insulin Signaling Balances Proliferation and Autophagy to Determine Follicle Stem Cell Lifespan. *Dev. Cell* **46**, 720–734.e6.
- Slaidina, M., Banisch, T. U., Gupta, S. and Lehmann, R.** (2020). A single-cell atlas of the developing Drosophila ovary identifies follicle stem cell progenitors. *Genes Dev.* **34**, 239–249.
- Slaidina, M., Gupta, S. and Lehmann, R.** (2021). A single cell atlas reveals unanticipated cell type complexity in Drosophila ovaries. *bioRxiv* 2021.01.21.427703.
- Song, X. and Xie, T.** (2003). Wingless signaling regulates the maintenance of ovarian somatic stem cells in Drosophila. *Development* **130**, 3259–3268.
- Tafesh-Edwards, G. and Eleftherianos, I.** (2020). JNK signaling in Drosophila immunity and homeostasis. *Immunol. Lett.* **226**, 7–11.
- Ulmschneider, B., Grillo-Hill, B. K., Benitez, M., Azimova, D. R., Barber, D. L. and Nystul, T. G.** (2016). Increased intracellular pH is necessary for adult epithelial and embryonic stem cell differentiation. *J. Cell Biol.* **215**, 345–355.
- Vied, C., Reilein, A., Field, N. S. and Kalderon, D.** (2012). Regulation of stem cells by intersecting gradients of long-range niche signals. *Dev. Cell* **23**, 836–848.
- Waldmann, R. et al.** H(+)-gated cation channels. *Annals of the New York Academy of Sciences* **868**, 67–76 (1999).
- Wang, Z. A., Huang, J. and Kalderon, D.** (2012). Drosophila follicle stem cells are regulated by proliferation and niche adhesion as well as mitochondria and ROS. *Nat. Commun.* **3**, 769.

Webb, B. A., Chimenti, M., Jacobson, M. P., & Barber, D. L. (2011). Dysregulated pH: A perfect storm for cancer progression. *Nature Reviews Cancer Nat Rev Cancer*, 11(9), 671-677.
doi:10.1038/nrc3110

Xiao, X., Lai, W., Xie, H., Liu, Y., Guo, W., Liu, Y., Li, Y., Li, Y., Zhang, J., Chen, W., et al. (2019). Targeting JNK pathway promotes human hematopoietic stem cell expansion. *Cell Discov* **5**, 2.

Zakrzewski, W., Dobrzyński, M., Szymonowicz, M. and Rybak, Z. (2019). Stem cells: past, present, and future. *Stem Cell Res. Ther.* **10**, 68.

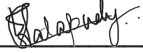
Zhang, Y. and Kalderon, D. (2000). Regulation of cell proliferation and patterning in *Drosophila* oogenesis by Hedgehog signaling. *Development* **127**, 2165–2176.

Zhang, Y. and Kalderon, D. (2001). Hedgehog acts as a somatic stem cell factor in the *Drosophila* ovary. *Nature* **410**, 599–604.

Publishing Agreement

It is the policy of the University to encourage open access and broad distribution of all theses, dissertations, and manuscripts. The Graduate Division will facilitate the distribution of UCSF theses, dissertations, and manuscripts to the UCSF Library for open access and distribution. UCSF will make such theses, dissertations, and manuscripts accessible to the public and will take reasonable steps to preserve these works in perpetuity.

I hereby grant the non-exclusive, perpetual right to The Regents of the University of California to reproduce, publicly display, distribute, preserve, and publish copies of my thesis, dissertation, or manuscript in any form or media, now existing or later derived, including access online for teaching, research, and public service purposes.

DocuSigned by:

7173074D1F974C2... Author Signature

12/16/2021
Date